17 Case Study: Evaluation of Hydrocarbon Sources in Guanabara Bay, Brazil

Maria de Fatima G. Meniconi and Silvana M. Barbanti

Petrobras S.A. Av. Jequitiba, 950, Cidade Universitaria, Ilha do Fundao, Rio de Janeiro, RJ, Brazil

17.1 Guanabara Bay and Hydrocarbon Apportioning

Hydrocarbons are present in worldwide environmental ecosystems, and their potential to cause adverse effects is usually associated with the concentration of polycyclic aromatic hydrocarbons (PAHs) (Neff, 1979). It must be emphasized, however, that these compounds may be introduced by many different mechanisms, including natural and anthropogenic processes (Philp, 1985; Kennicutt II et al., 1994; Kennicutt II, 1995; Simoneit, 1998; Lipatou and Albaigés, 1994).

Sources of naturally occurring PAH include natural fires, natural oil seepage, and recent biological or diagenetic processes — biogenic origin (Hites and Biemann, 1975; Youngblood and Blumer, 1975; Kennicutt II et al., 1994; Kennicutt II, 1995; Yunker et al., 2000; Yunker et al., 2002).

Anthropogenic sources of PAH are from direct runoff and discharges and indirect atmospheric deposition, i.e., from waste and releases/spills of petroleum and derivatives such as river runoff, sewage outfalls, maritime transport, pipelines, and combustion or pyrolysis of organic matter such as petroleum, coal, and wood (Lipatou and Albaigés, 1994; Budzinski et al., 1997; Elias et al., 2000; Wang et al., 1999a; Yunker et al., 2000; Yunker et al., 2002; Stout et al., 2001; Readman et al., 2002).

These compounds tend to interact with different types of environments and are subjected to many processes that lead to geochemical fates such as physical-chemical transformation, biodegradation, and photooxidation. Therefore, PAH characterization and the correlation of PAH to known or suspected sources become a challenge.

Another class of hydrocarbons present in worldwide environmental ecosystems is saturated hydrocarbons derived from fossil fuels (petroleum and its refined products). The trace organic compounds that provide information about source, maturation, and depositional environment are the so-called biological fossils or biomarkers (Eglinton et al., 1964; Eglinton and Calvin, 1967; Peters et al., 2005). Molecular parameters based on GC-MS analysis of these biomarkers, primarily terpanes and steranes, provide a method to relate the environment samples and crude oils. Therefore, the source of a certain sample containing fossil hydrocarbons can be determined by applying both biomarker ratios and profiles (see Chapter 3 herein).

Numerous studies for apportioning sources of PAH in the environment that apply diagnostic indexes based on chemical fingerprinting have been made mainly in temperate climate countries (Readman et al., 2002; Budzinski et al., 1997; Sicre et al., 1987; Gschwend and Hites, 1981). In the present study, the sources of PAH and other

hydrocarbons have been investigated on tropical estuarine ecosystem in the Guanabara Bay, Brazil, in which the scenarios of chronic and acute anthropogenic events were taken into consideration. Our study sought to identify hydrocarbon sources using both PAH diagnostic indexes and biomarker ratios, in combination with multivariate statistics based on principal component analysis (PCA) for intertidal and subtidal area sediments investigated in two campaigns: the years 2000 and 2003.

17.1.1 Regional Setting

Guanabara Bay is located in Greater Rio de Janeiro, where there exists a highly urban and industrialized ecosystem that receives intense chronic anthropogenic pollution and was the scene of an oil spill of 1300 m^3 of marine heavy fuel oil in January 2000 (Gabardo et al., 2001; Meniconi et al., 2002).

The bay is the centerpoint of a complex river drainage basin receiving water from about 50 rivers and channels and is used to dispose extensive municipal sewage, usually with minimal or no treatment, and receives urban runoff and industrial waste from the country's second largest city, with almost 10 million people (JICA, 1995; FEEMA, 1998). The bay drainage basin encompasses 15 districts with about 14,000 industries, 14 oil terminals, 2 commercial ports, 32 dock yards, more than 1000 gas stations, and 2 refineries. All of these inputs are responsible for an annual inflow of approximately 6.6 tons of hydrocarbons into the bay (FEEMA, 2005; Ferreira, 1995) (Figure 17-1). About 50% of the hydrocarbon input in the bay is due to the municipal sewage (17 m^3/s), while 27% corresponds to the urban runoff (Ferreira, 1995). Furthermore, 13,000 tonnes/day of solid waste are produced by the Great Rio de Janeiro area, of which 5,000 tonnes/day are ejected directly into the bay, forming a permanent trash line along the beaches and mangroves of the bay.

The bay has a water surface area of about 400 km^2 and a 156-km shoreline. It is a system with strong currents along the central channel due to tides and weaker currents in the north area of the bay. A shallow area of up to 5 m corresponds to about 46% of the total water surface of the bay. However, the average flushing time to renew 50% of the bay water is about 11 days (Kjerve et al., 1997). The central channel presents a faster renewal of the water due to the strong currents. On the other hand, in the north, northwest, and northeast areas of the bay, the renewal is low since the tidal currents are weaker than the central channel. Even so, the wind can increase the currents in the north, contributing to the renewal of water in this area. Spread along the shallow north region of the bay are approximately 350 fish traps, which form an important social economic aspect of the bay, the fishing communities.

The mangrove area, located on the northwest and northeast shorelines of the bay, is about 86 km^2, most of it significantly degraded (FEEMA, 2005; Amador, 1997). The largest part of the bay mangrove is situated inside an environmental protected area, established in the bay's northeast region.

17.1.2 January 2000 Heavy Fuel Oil Spill

The acute event of January 2000 was an accidental oil release of about 1300 m^3 of marine heavy fuel oil into the bay, due to a pipeline rupture at the Duque de Caxias Refinery of Petrobras, the Brazilian state oil company. An oil slick up to 56 km^2 formed on the bay surface (Bentz and Miranda, 2001), as can be seen in Figure 17-2. An extensive response for on-water oil recovery and shoreline cleanup was implemented following the accident. The main portion of the oil, transported by tidal currents and wind, reached the beaches and some islands in the north and northeast parts of the bay. Mangroves in the vicinity of the spill emission point also were affected.

Immediately following the oil spill response, 22 water and 57 sediment samples were collected from the Guanabara Bay area. These were characterized by measuring the concentrations of the *n*-alkanes, unresolved complex mixture (UCM), and polycyclic aromatic hydrocarbons (PAHs) biomarkers (terpanes and steranes) and by conducting toxicological assays for three species (*Artemia*

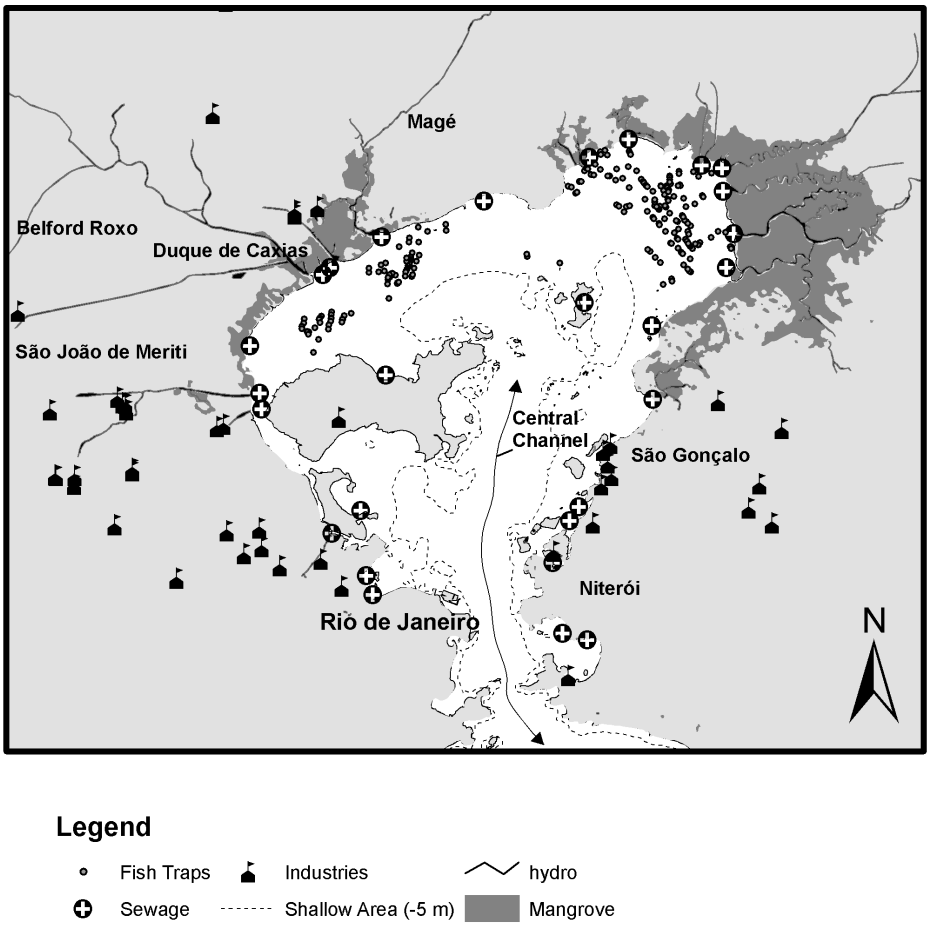

Figure 17-1 Social, economical, and physical characteristics of Guanabara Bay.

sp., Mysidium gracile, and *Vibrio fisheri* for Microtox® system). Composite fish tissue samples from two species were also analyzed, being chosen based on their abundance, marketability, and feeding habits. The fish were collected in the affected area and then analyzed and compared to the same species' frozen-dry samples collected 1 year prior to the spill by a local university (reference samples). The spilled heavy fuel oil was also characterized, revealing a relatively high density (0.9817 g/mL), 12°API, and viscosity (20°C) of 5313 cP. Approximately 21% of the fuel oil had evaporated after 72 hours of exposure, as calculated from the gas chromatographic comparison of the solvent-rinsed sand samples collected on the affected beaches and the original fuel oil. The biomarker analysis of the spilled marine heavy fuel oil confirmed that it was refined from a crude oil from a Brazilian marginal basin, as expected (Meniconi et al., 2002). Based on the results of this diagnostic study, no significant impact on the sediments, water column, and fish tissue of Guanabara Bay was observed due to the oil spill.

17.2 Methodology for Hydrocarbon Determination and Source Evaluation

17.2.1 Sampling Design

The strategy for this work on hydrocarbon source apportionment in the tropical estuarine ecosystem of Guanabara Bay was based on analysis of hydrocarbons in the sediments.

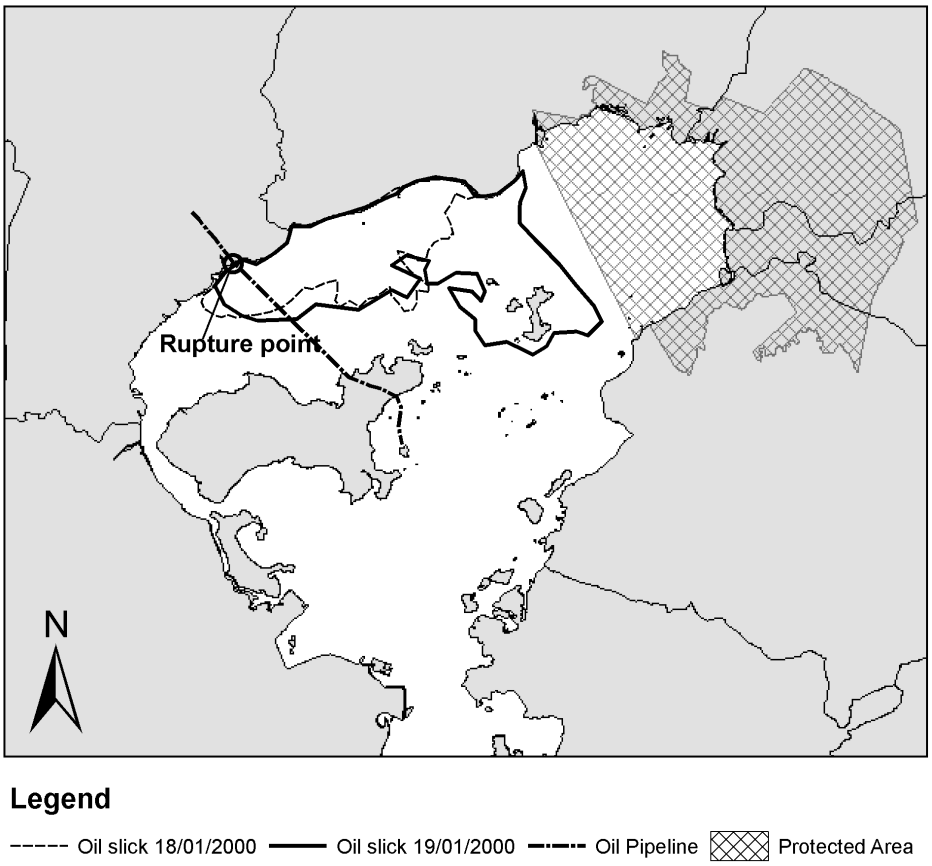

Figure 17-2 Oil slick after January 2000 oil spill accident in Guanabara Bay.

These data included a large number of compounds, including 38 PAH and 61 petroleum biomarkers (42 terpanes and 17 steranes). Among the 57 sediment stations analyzed immediately after the oil spill, 21 stations were chosen to develop the present study, representing areas potentially affected and unaffected by the spilled oil in January 2000 (Meniconi et al., 2002). The samples were collected using cores and dredges from the intertidal (stations T1 to T28) and subtidal regions (stations T31 to T57) of the bay. A subsample of the top 3 cm of each sediment was transferred into wide-mouth glass jars with Teflon caps and then freeze-stored for subsequent PAH analysis. Figure 17-3 shows the geographical location of the 21 sample stations in Guanabara Bay.

In the first sampling campaign (January 2000), the samples were collected from 21 stations (Figure 17-3), just 10 days after the accident. In the second sampling campaign (2003), the samples were collected from the same 21 stations studied in 2000, which permitted a good temporal investigation in the region.

17.2.2 Chemical Analysis

17.2.2.1 Sediment Sample Extraction

The majority of the samples was extracted following the methodology EPA Method 3540 (Soxhlet) and in some cases EPA 3550B (sonication). The sediment samples were thawed and homogenized, and a subsample (5 g) was mixed with sodium sulphate (1:4; w/w). Extraction was performed in a Soxhlet appa-

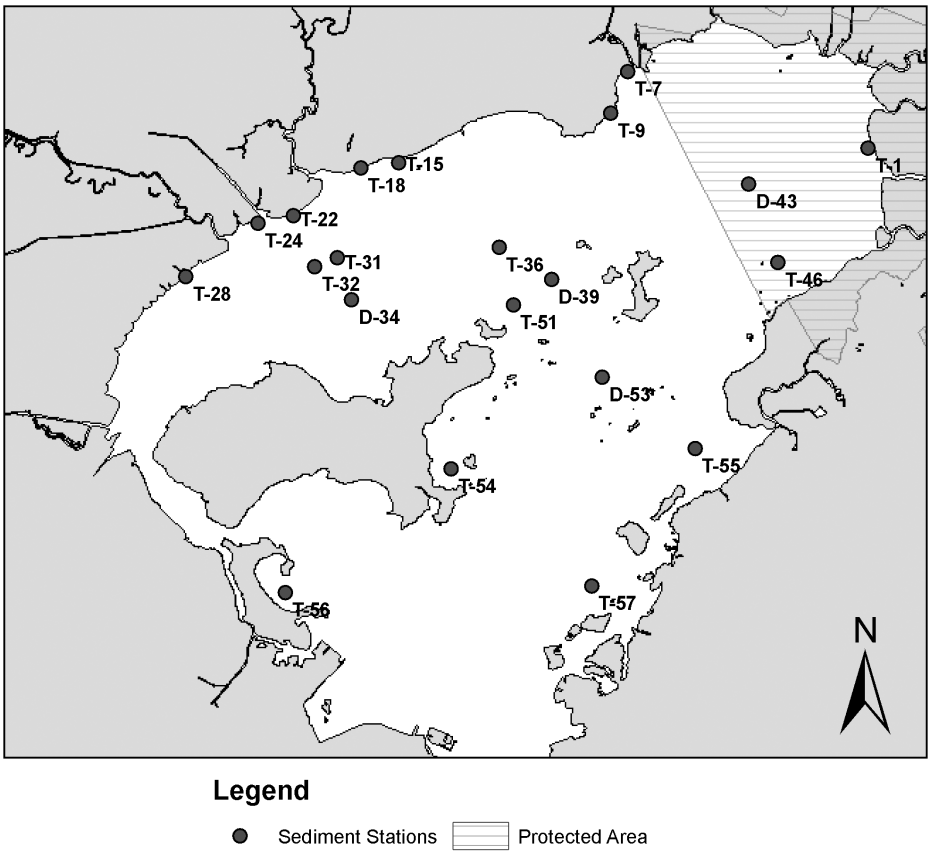

Figure 17-3 Geographical location of the 21 sediment stations in Guanabara Bay sampled in 2000 and 2003.

ratus for 4 hr with 200 mL of dichloromethane. Before the extraction, perdeuterated paraffins (*n*-eicosane-d_{42}, *n*-tetracosane-d_{50}, *n*-triacontane-d_{62}) and an aromatic hydrocarbon (p-terphenyl-d_{14}) were added to the sediment samples as surrogates. Sulfur was removed during extraction with granulated copper. A rotary evaporator was used to reduce the bulk extract volume to 5 mL, and then the solvent was changed to *n*-hexane in a Kuderna-Danish apparatus to a final volume of 1 mL.

17.2.2.2 Extract Cleanup

Sediment extracts were fractionated by adsorption chromatography, based on EPA Method 3630 modified. A column filled with 2.5 g of combusted sand (400°C), 20 g of 5% deactivated silicagel, 10 g of 1% deactivated basic alumina, 2.5 g of combusted sand, and 2.5 g of combusted sodium sulfate was used. The concentrated extract (1 mL) was carefully added to the top of the column, and the following fractions were collected: (1) 50 mL of *n*-hexane (aliphatic hydrocarbons, isoprenoids, and UCM); and (2) 200 mL of 1 : 1 dichloromethane : hexane (aromatic compounds). Both fraction volumes were reduced by rotary evaporator and a gentle stream of pure nitrogen to a final volume of 1 mL and stored under refrigeration until the analysis.

17.2.2.3 PAH Analysis of Sediment Samples

Gas chromatography-mass spectrometry (GC-MS) analysis for polycyclic aromatic hydrocarbons and their homologues followed the

EPA Method 8270-C, with modifications. This was carried out in an HP 5890-series II GC coupled to a Finnigan GCQ mass detector system. The mass spectrometer was operated in the electron impact (EI) mode (70 eV), and the data were acquired in full scan mode (15–400 amu). GC conditions were similar to those reported in aliphatic analyses, except for the oven temperature (40°C for 5 min and from 40 to 280°C at 8°C/min, with a final time hold of 30 min). Quantification was performed by internal standard method using a solution with acenaphthene-d_{10}, naphthalene-d_8, phenanthrene-d_{10}, chrysene-d_{12}, and perylene-d_{12}. The analytical method was certified by the extraction, in triplicate, of a marine sediment reference material and dry frozen mussels from NIST (SRM 1941a and SRM 2974), and blanks were periodically run to check contamination problems. The Canadian Association for Environmental Analytical Laboratories (CAEAL) certifies the laboratory twice a year. Detection limits were calculated as $1\,ng \cdot g^{-1}$ for sediment, dry weight.

17.2.2.4 Biomarkers

Biomarker analyses were performed by using a gas chromatograph coupled to a mass selective detector (MSD 5973N, Agilent), electron impact as ionization method, and selective ion monitoring as data acquisition mode for some diagnostic ions of these compounds [*m/z* 191, 177, 398, 412 for terpanes; *m/z* 217, 218 for steranes; *m/z* 231 for methylsteranes; *m/z* 259 for diasteranes and tetracyclic terpane polyprenoids (TPP); (Peters et al., 2005; Holba et al., 2000, 2003)]. GC conditions were similar to those reported in aromatic analyses, except for the oven temperature (55°C for 2 min, from 55 to 150°C at 15°C/min, from 150 to 320°C at 1.5°C/min, with a final time hold of 20 min). Quantification was performed by internal standard method using cholestane-d_4 or 5β-cholane. The analytical method was certified by analyzing the saturated hydrocarbon fraction of a reference crude oil, and running blanks periodically in order to check contamination problems.

17.2.3 Source Identification Techniques

The hydrocarbon source identification of the sediment samples from Guanabara Bay has been made by using different approaches: PAH diagnostic indexes, PAH multivariate analysis, and biomarker ratios, described in the following sections.

17.2.3.1 PAH Diagnostic Ratios

As previously reported, many PAH molecular ratios have been used to help to identify the PAH sources in environmental samples, whether petrogenic, biogenic, or pyrolytic (Youngblood and Blumer, 1975; Gschwend and Hites, 1981; Sicre et al., 1987; Lipatou and Albaigés, 1994; Kennicutt II, 1995; Budzinski et al., 1997; Baumard et al., 1998, Wang et al., 1999a; Yunker et al., 2000, 2002; Readman et al., 2002). The difficulty remains with the complexity of the samples themselves and the weathering effects on the composition of the original source of the compounds.

The use of parent PAH diagnostic ratios to interpret PAH sources is based on the relative stability of the PAH isomers, which have been evaluated from the relative heat of formation of the compounds. The heat of formation is the energy difference for each PAH isomer relative to the most stable isomer within a given molecular mass. The calculation of the heat of formation for a restricted mass (*m/z* 178, *m/z* 202, *m/z* 252, *m/z* 276) would prevent or minimize interferences such as differences in volatility, water solubility, and adsorption characteristics of the compounds (Yunker et al., 2000, 2002). It would be expected that ratios based on isomers with the highest heat of formation differences (i.e., greatest range in stability) would provide the highest discrimination capacity. For instance, the heat of formation differences between phenanthrene (Phe) and anthracene (An) and for fluoranthene (Fl) and pyrene (Py) are 5.48 kcal/mol and 20.58 kcal/mol, respectively, and the ratio Fl/Py would then have higher discrimination ability (Yunker et al., 2000, 2002). Software such as AM1 (Hyperchem, V4, 5, Hypercube, Inc., 419 Philip St.,

Waterloo, Ontario, Canada) and PCMODEL (V5.13, Serena Software, Box 3076, Bloomington, Indiana, USA) has been used to calculate the PAH heat of formation (Yunker et al., 2000).

The PAH molecular ratios used in this study covered parent and alkylated PAH homologues, which are listed below:

Parent PAH

- Phenanthrene/anthracene
- Fluoranthene/pyrene
- Anthracene/(anthracene + phenanthrene)
- Fluoranthene/(fluoranthene + pyrene)
- Indeno1,2,3-(cd)pyrene/(indeno1,2,3-(cd) pyrene + benzo(ghi)perylene)
- Perylene abundance index: Perylene/Σ (5-ring PAH)
  (5-ring PAH = BbFl + BkFl + BaPi + BePi + DBAn. See Table 17-1 for codes.)

Alkylated PAH

- Phenanthrene + anthracene/(phenanthrene + anthracene + C1phenanthrenes)
- Pyrogenic index: Σ (other 3–6-ring PAHs)/ Σ (5 alkylated PAH series)
  (5 alkylated PAH series = naphthalenes, fluorenes, dibenzothiophenes, phenanthrenes, and chrysenes)

The cross-plots used in this study included the PAH data from the 2000 and 2003 campaigns together and included data from four different oils: a heavy fuel; an Arabian oil; a light oil; and a diesel fuel.

17.2.3.2 PAH Multivariate Statistical Analysis

The multivariate analysis of the PAH concentration data applied in this study was based on principal component analysis (PCA) (Statistica version 5.0) in which the sample projections were separately plotted for surveys 2000 and 2003. However, some preprocessing of the data was conducted before applying PCA, namely:

- A half-limit concentration was used for nondetected compounds (0.5 ng/g).
- Each compound concentration was normalized to the total PAH concentration in the sample in order to prevent the influence of the wide range of sample concentrations.
- The normalized concentration data for each compound were reduced by the average and standard deviation for that compound within all of the samples.

17.2.3.3 Biomarker Diagnostic Ratios

Biomarker analyses were performed by using a gas chromatograph coupled to a mass selective detector (MSD 5973N, Agilent), electron impact as ionization method, and selective ion monitoring as data acquisition mode for some diagnostic ions of these compounds [*m/z* 191, 177, 398, 412 for terpanes; *m/z* 217, 218 for steranes; *m/z* 231 for methylsteranes; *m/z* 259 for diasteranes and tetracyclic terpane polyprenoids (TPP); (Peters et al., 2005; Holba et al., 2000, 2003)]. GC conditions were similar to those reported in aromatic analyses, except for the oven temperature (55°C for 2 min, from 55 to 150°C at 15°C/min, from 150 to 320°C at 1.5°C/min, with a final time hold of 20 min). Quantification was performed by internal standard method using cholestane-d_4 or 5β-cholane. The analytical method was certified by analyzing the saturated hydrocarbon fraction of a reference crude oil and running blanks periodically in order to check contamination problems.

17.3 Hydrocarbon Results for Guanabara Bay Sediments

17.3.1 PAH Quantification and Distribution

The concentration of individual PAH compounds and the sum of 16 EPA priority PAHs (Σ 16 PAHs) and the total 38 PAHs (Σ PAH) in the sediments collected in Guanabara Bay in 2000 (just after the oil spill) and in 2003 are shown in Tables 17-1 and 17-2, respectively. For both sampling campaigns, the concentration of total PAH varied significantly throughout the bay, ranging from 559 to 58,439 ng/g dry weight (median concentration: 4,877 ng/g)

Table 17-1 Results for the Individual PAH (ng/g dry weight)* of Sediment Samples from Guanabara Bay — Campaign 2000 and Studied Oils

Compound	*Code*	*Intertidal*							
		T1	*T7*	*T9*	*T15*	*T18*	*T22*	*T24*	*T28*
Naphthalene	**N**	6	2	2	12	7	5	12	4
1-Methylnaphthalene	**1MN**	3	19	6	24	6	45	6	2
2-Methylnaphthalene	**2MN**	6	26	7	48	15	67	21	9
C_2Naphthalenes	**C_2N**	77	363	303	364	122	1,695	211	226
C_3Naphthalenes	**C_3N**	3	983	944	440	163	6,236	524	88
C_4Naphthalenes	**C_4N**	19	1,189	1,377	338	172	6,738	1,214	97
Acenaphthalene	**Acl**	2	2	2	9	12	12	7	6
Acenaphthene	**Ace**	1	18	13	17	6	60	9	3
Fluorene	**F**	4	26	30	28	17	93	10	8
C_1Fluorenes	**C_1F**	5	160	199	74	55	601	80	24
C_2Fluorenes	**C_2F**	28	536	636	115	101	1,602	682	57
C_3Fluorenes	**C_3F**	30	585	815	111	109	1,748	1,987	83
Dibenzothiophene	**DBT**	5	52	89	42	30	162	31	11
C_1Dibenzothiophenes	**C_1DBT**	5	206	438	94	75	757	301	42
C_2Dibenzothiophenes	**C_2DBT**	22	441	963	170	145	1,352	2,160	100
C_3Dibenzothiophenes	**C_3DBT**	31	425	884	152	135	1,157	5,109	111
Phenanthrene	**Fe**	17	148	277	120	76	486	54	47
C_1Phenanthrenes	**C_1Fe**	21	490	888	187	141	1,579	549	93
C_2Phenanthrenes	**C_2Fe**	30	781	1,759	277	230	2,294	5,033	163
C_3Phenanthrenes	**C_3Fe**	28	666	1,479	231	204	1,900	10,485	148
C_4Phenanthrenes	**C_4Fe**	1	321	538	120	110	839	6,494	85
Anthracene	**An**	4	26	46	20	21	122	38	23
Fluoranthene	**Fl**	27	37	45	108	91	56	72	79
Pyrene	**Pi**	22	57	110	99	91	247	499	96
C_1Pyrenes	**C_1Pi**	2	106	222	112	118	547	2,679	81
C_2Pyrenes	**C_2Pi**	1	161	311	108	99	868	5,114	93
Benz (a) anthracene	**BaAn**	14	35	55	65	59	151	854	69
Chrysene	**C**	16	46	78	74	61	226	543	61
C_1Chrysenes	**C_1C**	15.1	94	215	101	90	777	5,298	96
C_2Chrysenes	**C_2C**	9	95	234	124	99	1,070	6,695	107
Benz(b)fluoranthene	**BbFl**	25	37	52	88	89	88	76	117
Benz(k)fluoranthene	**BkFl**	11	13	14	28	20	23	157	37
Benz(a)pyrene	**BePi**	19	29	48	62	47	87	370	81
Benz(e)pyrene	**BaPi**	16	25	33	52	45	89	451	66
Perylene	**Pe**	30	62	18	50	79	62	159	33
Indeno (1,2,3-cd)pyrene	**IPi**	17	22	27	60	58	72	79	71
Dibenz(a,h)anthracene	**DBAn**	6	8	12	26	16	57	188	23
Benzo(ghi)perylene	**BPe**	17	21	23	50	49	82	186	72
Σ 16HPA		207	526	819	866	719	1,866	3,235	797
Σ Total HPA		691	8,259	13,191	4,198	3,058	34,048	58,439	2,614

* Surrogate recovery: 68%–117% (average = 98%); n.d.: not detected.

for the 2000 campaign and 400 to 52,384 ng/g dry weight (median concentration: 3,603 ng/g) for the 2003 campaign. However, based on nonparametric analysis (Mann–Whitney, Kolmogorov–Smirnov, Kruskal–Wallis), it was verified there was no statistical difference in total PAH concentrations between the 2000 and 2003 samples.

In order to compare the data of this study to previously reported data for Guanabara Bay, it is necessary to evaluate only the Σ 16 EPA priority PAH results, which varied from 207 to 13,425 ng/g and 184 to 5,110 ng/g for the 2000 and 2003 campaigns, respectively (Tables 17-1 and 17-2). The range of these hydrocarbons' contamination was the same observed in previous sediment surveys conducted by Lima (1996) (1,564 to 18,438 ng/g), Hamacher (1996) (554 to 1,894 ng/g), and Chalaux (1995) (1,051 to 5,861 ng/g).

Subtidal													*Oil*			
T31	*T32*	*T36*	*T46*	*T51*	*T54*	*T55*	*T56*	*T57*	*D34*	*D39*	*D43*	*D53*	*Ar.*	*A.L.*	*MF 380*	*D.M.*
20	55	16	5	16	3	<1	45	8	8	83	3	71	1,452	115	478	304
10	39	9	8	10	<1	<1	28	2	6	21	<1	37	18,852	416	1,913	1,339
35	84	33	27	25	4	5	89	8	6	67	<1	93	10,558	426	3,349	1,983
234	629	294	166	294	9	100	315	16	328	218	189	166	61,032	2,166	11,304	7,237
92	1,458	55	148	56	7	56	163	10	55	132	24	91	55,182	2,303	12,259	8,397
84	1,536	50	109	59	9	41	156	<1	56	120	11	76	28,911	1,547	6,130	4,614
13	7	86	10	77	3	55	147	4	35	507	6	315	470	16	79	n.d.
4	15	7	3	8	<1	7	28	3	5	29	<1	10	1,886	4	316	55
13	38	21	18	18	2	18	55	5	10	82	6	59	1,405	40	300	200
47	192	31	60	10	2	23	87	6	17	88	11	66	3,725	158	787	474
73	618	43	90	114	4	33	255	8	41	128	28	118	5,530	322	1,203	887
122	971	67	103	211	10	45	326	9	108	217	22	163	3,934	477	860	934
25	85	13	34	13	<1	16	31	3	10	24	6	53	805	225	245	196
58	392	43	77	47	4	40	76	7	37	73	15	84	1,564	641	601	430
127	1,126	80	123	138	9	66	179	10	93	297	19	202	895	1,137	727	500
334	1,343	118	101	230	17	82	248	11	151	398	18	263	365	949	525	349
57	217	75	62	68	15	104	168	40	59	204	28	168	4,914	77	898	782
139	923	95	112	111	12	101	189	26	95	411	28	259	8,052	295	1,619	1,555
272	1,815	134	136	248	15	112	286	23	175	846	35	480	4,921	461	1,325	1,911
474	1,948	165	110	268	22	105	312	18	40	855	27	448	1,273	414	720	1,474
537	1,068	60	50	192	18	65	276	11	191	341	12	196	260	208	294	554
59	65	56	25	39	5	51	111	15	38	251	9	157	1,033	13	165	50
78	113	149	65	192	29	188	248	77	115	468	40	532	27	<0.5	6	4
138	225	218	72	227	34	221	629	84	171	921	51	791	125	9	67	44
280	453	270	57	337	21	192	667	53	210	1,772	33	1,209	84	39	160	145
544	661	224	48	306	20	133	561	29	225	1,505	25	879	23	94	211	172
126	126	198	57	170	23	199	281	65	102	1,025	36	927	1	n.d.	30	19
89	183	179	56	175	21	161	176	57	85	875	30	776	2	n.d.	54	63
457	517	291	57	264	21	187	383	40	165	1,452	25	1,105	2	34	158	110
764	673	241	42	191	18	119	231	21	179	690	14	620	1	46	172	9
133	107	278	76	286	44	323	528	55	184	2,153	53	1,246	n.d.	<0.5	5	4
33	101	114	38	129	17	109	198	23	70	838	20	478	n.d.	<0.5	n.d.	n.d.
122	88	286	66	272	34	274	434	51	128	1,161	38	1,382	n.d.	9	14	11
110	96	144	47	167	25	170	309	29	147	2,151	31	561	n.d.	n.d.	9	5
94	89	67	50	68	9	63	91	14	47	315	95	227	n.d.	n.d.	3	<1,5
127	73	298	77	228	36	256	464	51	148	1,660	35	1,120	n.d.	n.d.	n.d.	<1,5
110	43	119	38	70	10	77	144	21	43	551	8	485	n.d.	n.d.	1	<1,5
143	68	252	68	215	27	223	464	41	146	1,628	21	883	n.d.	n.d.	3	<1,5
1,264	1,524	2,352	735	2,189	303	2,267	4,119	600	1,366	13,425	381	9,399	11,314	282	2,415	1,534
6,174	18,240	4,877	2,487	5,398	559	4,019	9,816	952	3,730	24,555	1,048	16,793	217,282	12,638	46,990	34,807

The comparison of this study data with data from other estuarine and coastal regions in the world reported in the literature is presented in Table 17-3. The PAH concentrations in Guanabara Bay sediments collected at the time of the oil spill and 3 years after it are in a similar range as found at various international estuarine marine sites, with and without correlation to oil spills. These data suggest that the PAH concentrations in Guanabara sediments are not obviously related to the oil spill event, but rather to long-term anthropogenic input.

Considering the distribution of PAH of Guanabara Bay sediment samples for the 2000 and 2003 surveys, it was found, in general, a higher alkylated PAH contribution for intertidal samples from the 2000 campaign, where oil was observed. This can be observed in Figure 17-4, where all series of weathered alkylated

Table 17-2 Results for the Individual PAH (ng/g dry weight)* of Sediment Samples from Guanabara Bay — Campaign 2003 and Studied Oils

Compound	*Code*	*Intertidal*							
		T1	*T7*	*T9*	*T15*	*T18*	*T22*	*T24*	*T28*
Naphthalene	**N**	4	1	3	5	6	6	13	6
1-Methylnaphthalene	**1MN**	2	<1	2	8	3	4	5	20
2-Methylnaphthalene	**2MN**	3	1	4	7	5	11	16	10
C_2Naphthalenes	**C_2N**	32	5	18	64	35	55	100	133
C_3Naphthalenes	**C_3N**	12	12	20	102	42	91	113	206
C_4Naphthalenes	**C_4N**	7	32	33	120	60	143	219	319
Acenaphthalene	**Acl**	2	2	3	4	5	7	7	<2.5
Acenaphthene	**Ace**	<1	<1	2	21	2	2	3	3
Fluorene	**F**	2	1	4	13	6	8	8	9
C_1Fluorenes	**C_1F**	4	4	8	50	22	28	35	52
C_2Fluorenes	**C_2F**	5	23	20	81	46	75	212	184
C_3Fluorenes	**C_3F**	9	48	29	118	59	136	1,003	334
Dibenzothiophene	**DBT**	3	2	4	13	6	10	13	11
C_1Dibenzothiophenes	**C_1DBT**	5	7	5	41	18	44	117	47
C_2Dibenzothiophenes	**C_2DBT**	7	26	29	128	50	163	801	136
C_3Dibenzothiophenes	**C_3DBT**	7	56	37	173	75	403	3,350	180
Phenanthrene	**Fe**	12	7	25	42	21	27	30	40
C_1Phenanthrenes	**C_1Fe**	12	17	28	84	36	79	205	121
C_2Phenanthrenes	**C_2Fe**	11	60	58	194	75	249	1,723	318
C_3Phenanthrenes	**C_3Fe**	8	20	84	245	88	569	6,493	408
C_4Phenanthrenes	**C_4Fe**	3	72	56	169	63	588	8,491	257
Anthracene	**An**	3	2	7	10	5	17	31	6
Fluoranthene	**Fl**	23	28	65	99	58	52	56	35
Pyrene	**Pi**	25	48	57	52	49	84	625	69
C_1Pyrenes	**C_1Pi**	12	56	47	97	63	244	3,146	119
C_2Pyrenes	**C_2Pi**	7	71	43	72	49	496	7,638	173
Benz (a) anthracene	**BaAn**	17	20	38	41	24	48	622	10
Chrysene	**C**	13	19	32	42	30	55	467	35
C_1Chrysenes	**C_1C**	12	28	30	54	39	258	5,349	61
C_2Chrysenes	**C_2C**	5	51	34	60	43	488	8,711	61
Benz(b)fluoranthene	**BbFl**	23	22	46	78	48	82	279	21
Benz(k)fluoranthene	**BkFl**	10	8	15	21	13	20	41	5
Benz(a)pyrene	**BePi**	19	14	17	37	24	81	777	17
Benz(e)pyrene	**BaPi**	15	18	33	38	18	65	684	10
Perylene	**Pe**	32	24	13	41	51	72	215	167
Indeno (1,2,3-cd)pyrene	**IPi**	16	16	27	45	30	68	116	8
Dibenz(a,h)anthracene	**DBAn**	4	5	8	14	8	35	301	<2.5
Benzo(ghi)perylene	**BPe**	15	15	26	37	26	71	372	11
Σ 16PAH		184	212	388	560	349	647	3,653	269
Σ Total PAH		400	838	1,004	2,516	1,303	4,931	52,384	3,603

* Surrogate recovery: 61%–119% (average = 101%); n.d.: not detected.

PAHs are predominant in the 2000 survey for samples T7, T9, and T22.

On the other hand, for both campaigns, a predominance of four- and five-ring PAHs over other compounds for subtidal stations was observed, either inside the influence of the oil spill slick (T36, T51, D53) or beyond the influence (T55, T56, and T57), as can be seen in Figure 17-5(a) and (b), respectively. This feature is typical for estuarines near urban areas in which the PAHs in runoff are associated with combustion-derived particulate matter (Stout et al., 2004).

17.3.2 Hydrocarbon Source Identification

17.3.2.1 PAH Diagnostic Ratios

Comparisons of the set of PAH diagnostic ratios (above) were used to distinguish the

Subtidal													*Oil*			
T31	*T32*	*T36*	*T46*	*T51*	*T54*	*T55*	*T56*	*T57*	*D34*	*D39*	*D43*	*D53*	*Ar.*	*A.L.*	*MF 380*	*D.M.*
7	13	20	19	7	20	24	45	<1	6	10	<1	49	1,452	115	478	304
6	40	22	10	11	11	8	17	1	5	13	n.d.	13	18,852	416	1,913	1,339
18	70	3	28	7	22	27	60	2	12	<1	n.d.	39	10,558	426	3,349	1,983
121	1,091	112	346	73	212	221	307	21	57	139	16	110	61,032	2,166	11,304	7,237
236	3,657	44	133	34	56	59	118	9	71	104	20	53	55,182	2,303	12,259	8,397
453	4,685	33	76	29	54	34	78	10	78	142	14	41	28,911	1,547	6,130	4,614
5	2	73	6	5	36	57	186	9	23	6	6	120	470	16	79	n.d.
3	16	6	2	80	9	10	32	2	4	3	<1	12	1,886	4	316	55
10	70	15	14	13	18	18	47	5	10	8	5	29	1,405	40	300	200
54	560	15	45	19	23	19	51	6	23	12	10	33	3,725	158	787	474
256	2,204	23	55	36	35	30	66	18	57	77	13	52	5,530	322	1,203	887
620	4,116	44	54	62	77	36	120	25	98	113	16	87	3,934	477	860	934
23	100	10	18	8	15	14	25	3	13	12	7	16	805	225	245	196
87	921	25	44	21	38	28	58	7	28	53	12	<1	1,564	641	601	430
447	2,087	59	71	84	94	56	116	24	88	140	18	131	895	1,137	727	500
872	2,170	82	55	165	155	59	140	49	147	154	15	224	365	949	525	349
62	300	70	49	51	103	99	154	39	53	52	24	102	4,914	77	898	782
223	1,657	85	83	97	109	100	181	32	88	104	26	119	8,052	295	1,619	1,555
189	3,905	119	96	60	129	111	209	51	146	199	4	233	4,921	461	1,325	1,911
1,216	2,191	120	71	270	168	96	197	35	187	185	3	295	1,273	414	720	1,474
964	2,376	73	29	138	90	48	106	27	138	121	<1	155	260	208	294	554
29	70	49	10	33	43	48	145	11	24	25	7	66	1,033	13	165	50
30	93	147	42	185	224	178	280	57	107	93	38	222	27	<0.5	6	4
126	393	181	49	224	248	262	885	85	117	131	42	383	125	9	67	44
268	921	211	35	329	217	259	755	80	125	118	24	609	84	39	160	145
547	1,529	165	26	298	168	155	435	62	157	149	16	516	23	94	211	172
75	94	170	29	219	155	227	392	62	71	86	28	351	1	n.d.	30	19
73	190	151	31	199	150	198	315	60	69	82	28	316	2	n.d.	54	63
130	435	225	31	246	175	216	506	53	112	138	25	533	2	34	158	110
486	757	153	25	159	132	134	256	29	159	175	17	316	1	46	172	9
69	46	305	55	411	200	311	825	84	126	86	55	373	n.d.	<0.5	5	4
15	9	118	23	144	81	110	335	29	46	36	19	136	n.d.	<0.5	n.d.	n.d.
49	36	284	44	267	178	270	686	69	91	73	38	355	n.d.	9	14	11
66	47	169	36	374	135	168	484	52	88	59	29	257	n.d.	n.d.	9	5
53	58	60	46	66	41	61	139	16	37	25	65	75	n.d.	n.d.	3	<1.5
43	48	205	34	310	184	177	455	55	128	60	40	334	n.d.	n.d.	n.d.	<1.5
19	nd	60	11	76	56	58	144	16	39	24	13	127	n.d.	n.d.	1	<1.5
44	58	153	32	281	169	147	386	48	117	57	36	301	n.d.	n.d.	3	<1.5
675	1,448	1,891	443	2,611	1,829	2,090	5,110	614	1,028	818	368	3,177	11,314	282	2,415	1,534
7,993	37,014	3,856	1,861	5,090	4,028	4,130	9,734	1,242	2,944	3,063	726	7,182	217,282	12,638	46,990	34,807

sources of the Guanabara Bay sediment samples including the parent PAH and the alkyl PAH ratios.

The double-ratio plot of phenanthrene/anthracene (Phe/An) versus fluoranthene/pyrene (Fl/Py) has been frequently used to distinguish a mixture of petrogenic and pyrolytic input for sediments (Baumard et al., 1998; Tam et al., 2001; Readman et al., 2002; Ke et al., 2002) despite the low discrimination capacity of Phe/An. Figure 17-6 depicts this parental ratio diagram for Guanabara Bay samples collected in both campaigns, 2000 and 2003, plotted together with the January 2000 oil spill sample (MF 380 derived from a crude oil from a Brazilian marginal basin), an Arabian crude oil (AL), frequently used in Brazilian refineries, a light oil (Ar), and a diesel fuel (DM) produced in a refinery from the south of the country. It was observed that this double-ratio

Table 17-3 Literature Data on PAH Concentration (ng/g dry weight) of Sediments from Various Coastal Sites in the World

Location	*Number of PAH Analyzed*	*Concentration Range (ng/g)*	*References*
Casco Bay, USA	23	16–20,748	Kennicutt et al., 1994
San Diego, USA	36	80–20,000	Anderson et al., 1996
San Francisco Bay, USA	17	2,653–27,680	Pereira et al., 1996
San Francisco Bay (Alameda), USA	43	751–11,059	Stout et al., 2004
Masan Bay, Korea	16	41–1,100	Khim et al., 1999
Gironde & Arcachon Bay, France	14	3.5–853	Sicre et al., 1987
Sarasota Bay, USA	11	17–26,771	Sherblom et al., 1995
Brisbane River Estuary, Australia	17	2,840–13,470	Kayal & Connell, 1989
Mersey Estuary, UK	13	5,310	Readman et al., 1986
Tamar Estuary, UK	13	8,630	Readman et al., 1986
Toulon Harbour, France	14	8,400	Baumard et al., 1998
Portland Harbor, USA	43	860–20,644	Stout et al., 2004
Eagle Harbor, WA, USA	43	8,524–80,913	Stout et al., 2004
Cerritos Channel, Los Angeles, USA	23	10,000	Brown et al., 1998
Jiulongjiang Estuary, China	21	515–1,522	Witt & Siegel, 2000
Baoshan, Shangai, China	7	61–7,618	Xu et al., 2001
Yalujiang Estuary, North China	10	79–1,500	Wu et al., 2003
Minjiang River Estuary, China	16	112–887	Zhang et al., 2004
Deep Bay (mudflat), China	16	238–416	Zhang et al., 2004
Masan Bay, Korea	24	207–2,670	Yim et al., 2005
Pearl River Estuary, China	16/47	156–10,810	Fu et al., 2001; Bixian et al., 2001
Pearl River Estuary, China	15	94–4,300	Fung et al., 2005
Rio de la Plata Estuary, Argentina	18	50–555,000	Colombo et al., 1989
Daya Bay, Hong Kong, China	16	115–1,134	Zhou & Maskaoui, 2003
Channel of Rio de la Plata (after oil spill), Argentina	16	10–70,000	Colombo, 2000
Guanabara Bay (campaign 2000)	16	207–13,425	This study
	38	559–58,439	
Guanabara Bay (campaign 2003)	16	184–3,653	
Brazil	38	400–52,384	

plot does not give a strong interpretation of PAH sources although some intertidal sediments (T1, T9, T15, and T18) showed pyrogenic characteristics, i.e., Fl/Py higher than 1 and Phe/An less than 10, as observed in the studies of Budizinski et al., 1997; Baumard et al., 1998; and Readman et al., 2002. All other samples of Guanabara Bay and even the studied oils (MF 380, the Arabian oil, the light oil, and the diesel fuel) presented mixed features in this double-ratio plot, fitting in its bottom left quadrant. This was expected since the pair of compounds phenanthrene and anthracene has small relative difference in thermodynamic stability between isomers, and this ratio is likely to be less effective in identifying PAH sources (Yunker et al., 2000).

A similar parental double ratio plot proposed by Yunker and collaborators (2000): anthracene/(anthracene + phenanthrene) versus fluoranthene/(fluoranthene + pyrene) was studied in order to verify the ratio's ability to distinguish between combustion and petroleum inputs. This can be seen in Figure 17-7. It must be highlighted that this proposed ratio Fl/(Fl + Py) has a more detailed boundary for combustion sources: it distinguishes fuel combustion from grass/wood/coal combustion. The boundaries for Fl/(Fl + Py) and other ratios that will be presented in this study were

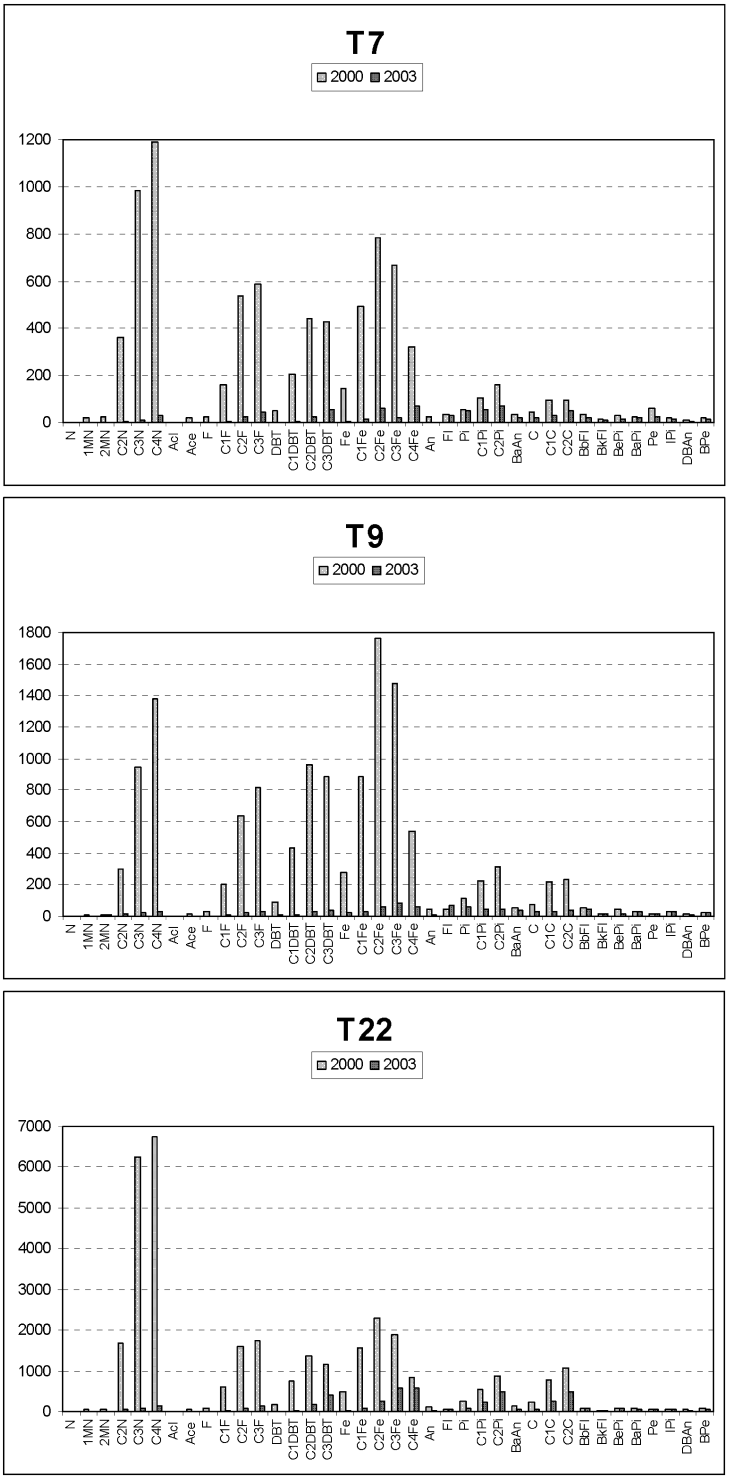

Figure 17-4 Predominance of alkylated PAH for intertidal samples from Guanabara Bay 2000 survey in relation to 2003.

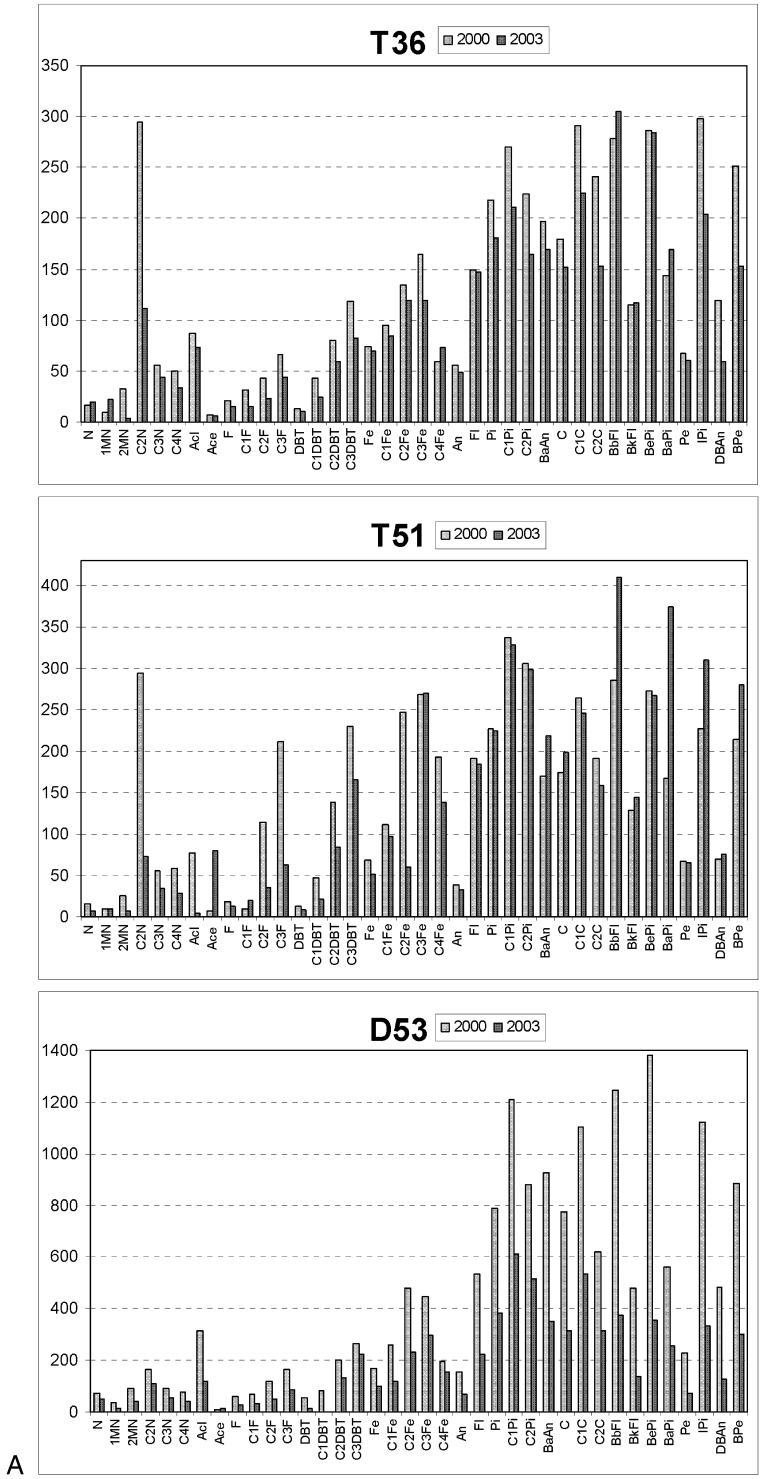

Figure 17-5 Predominance of four- and five-ring PAH for subtidal samples from Guanabara Bay for 2000 and 2003 campaigns. (a) Inside the influence of the oil spill slick; (b) outside the influence of the oil spill slick.

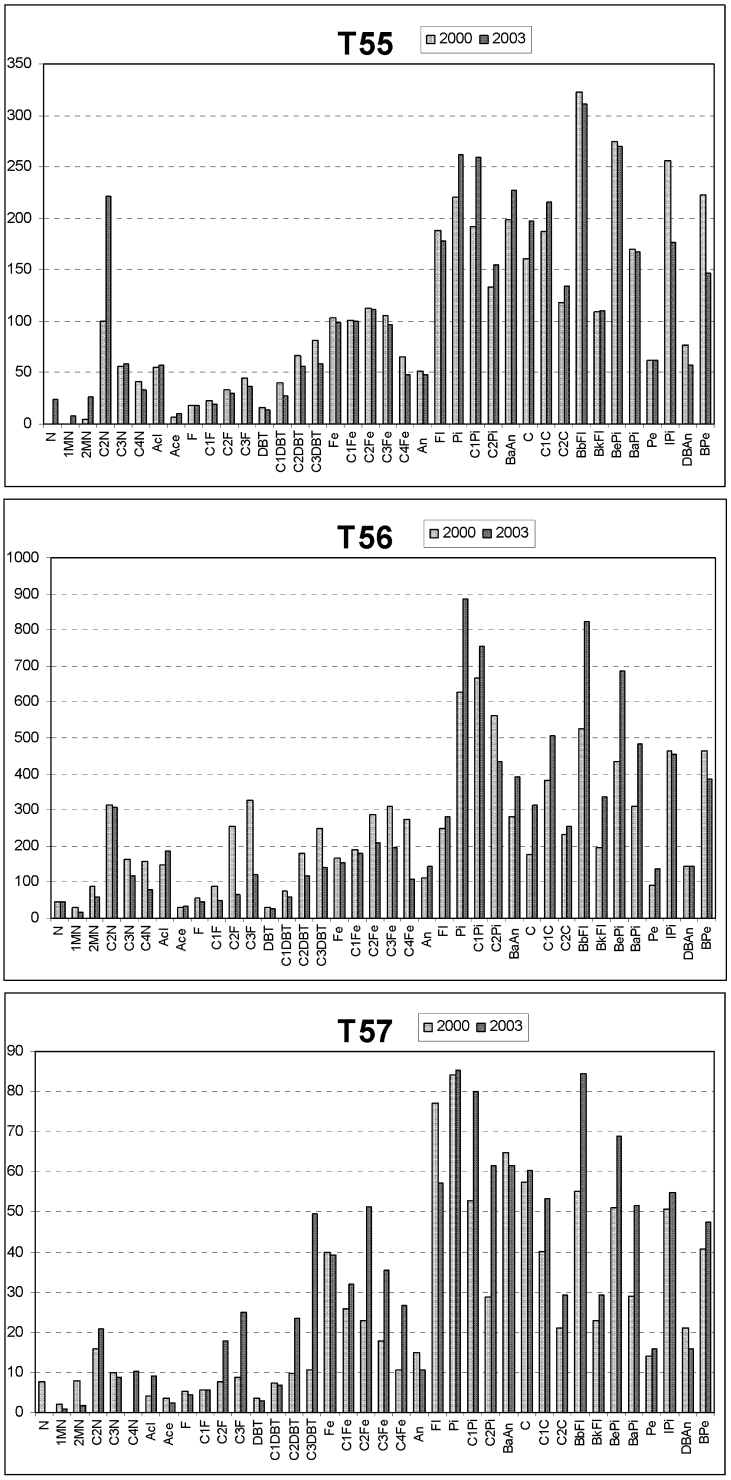

B

Figure 17-5, continued

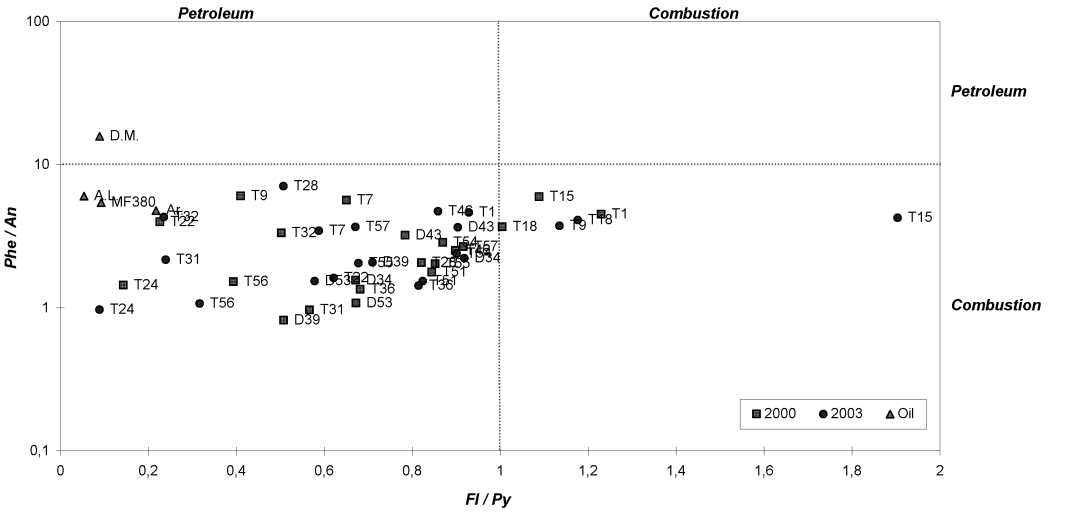

Figure 17-6 PAH cross-plot of phenanthrene/anthracene versus fluoranthene/pyrene for Guanabara Bay sediments and MF 380, Arabian oil (AL), light oil (Ar), and diesel oil (DM).

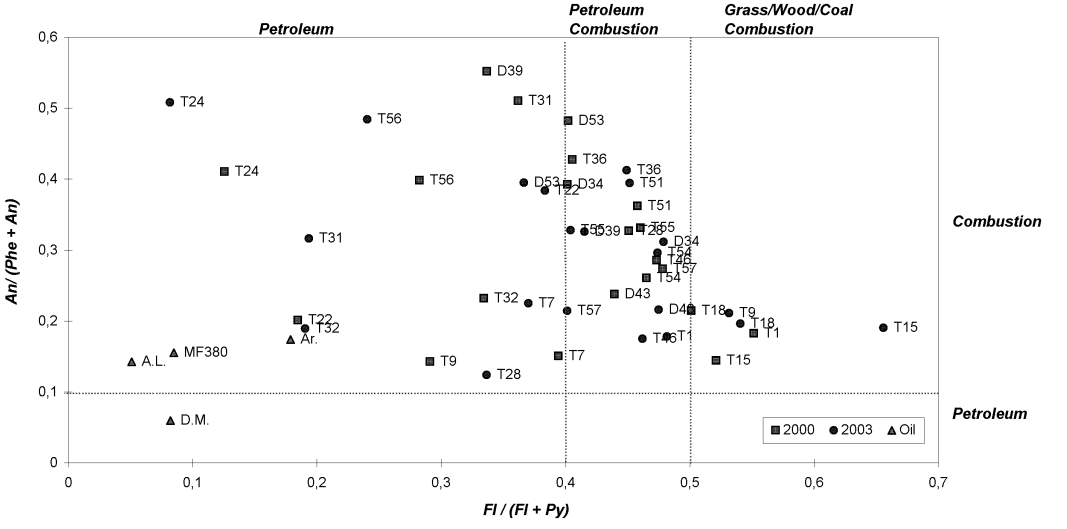

Figure 17-7 PAH cross-plot of anthracene/(anthracene + phenanthrenes) versus fluoranthene/(fluoranthene + pyrene) for Guanabara Bay sediments from campaigns 2000 and 2003 and MF 380, Arabian oil (AL), light oil (Ar), and diesel oil (DM).

established by Yunker and collaborators (2000) and were based on more than 40 studies from international literature, encompassing results of about 250 samples, including several types of petroleum, single sources of combustions (coal, wood, grass, oil), and environmental samples (bush fires, tunnels dust, road dust, urban air).

The low efficiency to determine PAH sources for anthracene and phenanthrene compounds was confirmed, which included all samples from Guanabara Bay in the category

of pyrogenic characteristics (An/An + Phe higher than 0.1).

On the other hand, the ratio Fl/(Fl + Py) has shown a higher ability to distinguish combustion and petroleum inputs, separating the Guanabara Bay samples into two clusters: Fl/(Fl + Py) less than 0.4 for samples with petrogenic characteristics; and Fl/(Fl + Py) higher than 0.4 for those with combustion sources (Yunker et al., 2000, 2002). As mentioned before, the ratio showed a more sophisticated discrimination ability for the samples: the differentiation between wood/grass/coal combustion (ratio higher than 0.5) and petroleum combustion features (ratio range between 0.4 and 0.5) (Figure 17-7).

This was also observed in Fraser River samples (Yunker et al., 2000, 2002). The PAH pair fluoranthene and pyrene has a higher relative difference in thermodynamic stability between isomers than phenanthrene and anthracene, therefore being more effective to determine PAH sources. In general, the majority of samples from subtidal stations (from T31 on) presented combustion characteristics.

Other double-ratio plots reported in the literature have been analyzed for Guanabara Bay samples, and it was verified that the parental ratio indeno1,2,3-(cd)pyrene/(indeno1,2,3-(cd)pyrene + benzo(ghi)perylene) presented low efficiency to identify PAH sources (Figure 17-8). The majority of the samples corresponded to predominant combustion features, including the Arabian and light oils. Only the MF 380 was identified as a petroleum derivative sample.

In addition to the parental Fl/(Fl + Py) ratio, it was observed that the alkylated ratio phenanthrene + anthracene/(phenanthrene + anthracene + C1phenanthrene) (Yunker et al., 2000) has also exhibited high source discrimination capacity for Guanabara Bay samples. This can be seen in Figure 17-9, in which this ratio was plotted against Fl/(Fl + Py). The double-ratio plot of these two most promising ratios showed the highest ability to distinguish between pyrogenic and petrogenic sources in this study.

It could be observed that the ratio Phe + An/(Phe + An + C1Phe) separated samples into two clusters. Samples with a ratio higher than 0.5 would correspond to a combustion-dominant source; less than 0.5 could indicate petroleum or combustion characteristics,

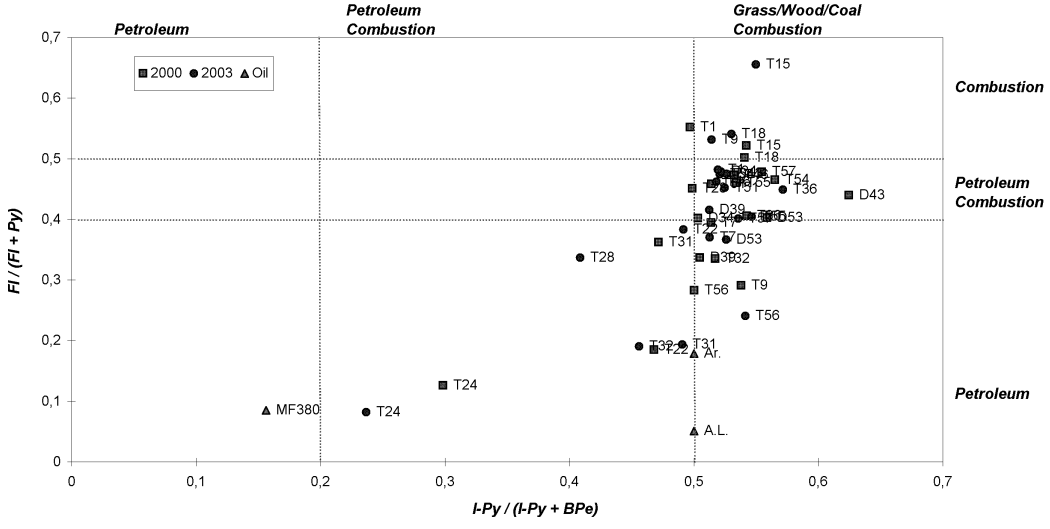

Figure 17-8 PAH cross-plot of indeno1,2,3-(cd)pyrene/(indeno1,2,3-(cd)pyrene + benzo(ghi)perylene) versus fluoranthene/(fluoranthene + pyrene) for Guanabara Bay sediments from campaigns 2000 and 2003 and MF 380, Arabian oil (AL), light oil (Ar), and diesel oil (DM).

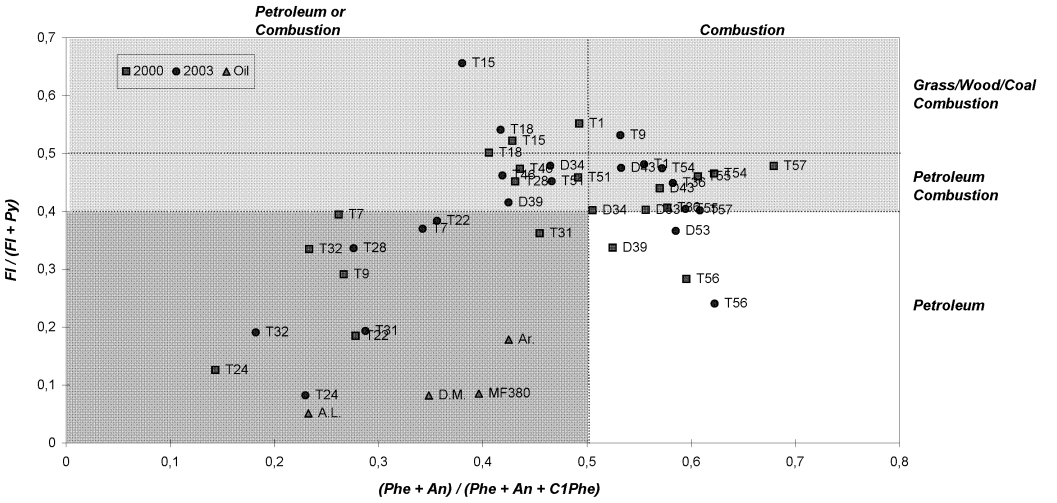

Figure 17-9 PAH cross-plot of fluoranthene/(fluoranthene + pyrene) versus phenanthrene + anthracene/(phenanthrene + anthracene + C1phenanthrenes) for Guanabara Bay sediments from campaigns 2000 and 2003 and MF 380, Arabian oil (AL), light oil (Ar), and diesel oil (DM). Interpretive guidelines based upon Yunker et al. (2000).

as claimed by Yunker and collaborators (2000).

As mentioned before, the ratio Fl/(Fl + Py) has shown the ability to distinguish between combustion and petroleum inputs, separating the samples into two clusters: ratio less than 0.4 for samples with petrogenic characteristics and ratio higher than 0.4 for those with combustion sources (petroleum combustion and grass/wood/coal combustion).

So, it was observed that combustion was the dominant source for samples with Fl/(Fl + Py) higher than 0.4 and Phe + An/(Phe + An + C1Phe) higher than 0.5 for Guanabara Bay samples. This corresponded to the top right quadrant of the diagram in Figure 17-9 (light shaded area). Samples with those characteristics were D34, T36, D43, D53, T54, T55, T57, for the 2000 survey, and T1, T9, T36, D43, T54, T55, T57, for the 2003 survey. This double-ratio source interpretation provided a good correlation with the whole PAH patterns for these samples, as can be seen in Figure 17-5(a) and (b), in which the PAH distribution of some samples is displayed, showing a strong pyrogenic signature.

Samples with Fl/(Fl + Py) less than 0.4 (petroleum input) and Phe + An/(Phe + An + C1Phe) less than 0.5 (could have petroleum or combustion input) would then correspond to a petroleum-dominant source. This corresponded to the bottom left quadrant of the diagram with a dark shaded area (Figure 17-9). For Guanabara Bay, the samples with those characteristics were T7, T9, T22, T24, T31, T32, for the 2000 survey, and T7, T22, T24, T28, T31, T32, for the 2003 survey. It should be emphasized that the analyzed oil samples (MF 380, Arabian oil, light oil, and diesel fuel) were clearly allocated in the bottom left quadrant of the diagram, confirming their petrogenic character. Once again, it could be verified that this source interpretation based on PAH double ratios comes to reflect the full PAH patterns for these samples (with petrogenic signature), as can be seen in Figure 17-4.

On the other hand, samples with Fl/(Fl + Py) higher than 0.4 (combustion input) and Phe + An/(Phe + An + C1Phe) less than 0.5 (petroleum or combustion input) would therefore correspond to a combustion-dominant source. This corresponded to the top left quadrant of the diagram of Figure 17-9 with the samples T1, T15, T18, T28, T51, for the 2000 survey, and samples T15, T18, T34, D39, T46, for the

2003 survey (light shaded area in the diagram). In this way, a great part of Guanabara Bay samples showed pyrolytic characteristics, allocated in both left and right top quadrants of the diagram. This covered samples from stations T1, T9, T15, T18, T28, D34, T36, D39, T43, T46, T51, T54, T55, and T57.

The exception for the double-ratio Fl/(Fl + Py) versus Phe + An/(Phe + An + C1Phe) to distinguish pyrogenic and petrogenic sources for Guanabara Bay samples was found in the bottom right quadrant of the diagram of Figure 17-9. The PAH source for stations D39 (survey 2000), D53 (survey 2003), and T56 (surveys 2000 and 2003) could not be clearly identified, probably due to a mixture of petrogenic and pyrolytic inputs and weathering processes.

A temporal investigation on the bay can be made comparing data from the 2000 and 2003 surveys obtained for the ratio Fl/(Fl + Py) versus Phe + An/(Phe + An + C1Phe). No significant changes were confirmed on the class of predominant source of the samples in this study. Only samples T9 and T28 have shown different PAH source contribution from one campaign to the other. In the 2000 survey, sample T9 has shown predominant petrogenic characteristics, corroborating the visual inspection of the intertidal region reached by the oil after the oil spill, where it was very affected.

Another compositional index used to differentiate the pyrogenic and petrogenic PAHs is the pyrogenic index reported by Wang et al. (1999b), which is defined as the ratio of the other EPA priority 3–6-ring PAHs to the total of 5 target alkylated PAH homologues [Σ (other 3–6-ring PAH)/Σ (5 alkylated PAH series)]. Based on more than 60 oils and petroleum products analyzed by Wang and collaborators, values up to 0.05 for the pyrogenic index unambiguously indicated the contribution of oil and refined products in the samples, while values greater than 0.5 (ratio increased tenfold) indicated combustion-derived sources for the samples. This ratio yielded high accuracy and consistency once the interference was minimized from concentration fluctuations from one compound to another.

For Guanabara Bay samples, this ratio (Figure 17-10) showed a good resolution, covering mostly subtidal samples and exceptionally T1 (from both the 2000 and 2003 surveys) and T9 (from the 2003 survey) with pyrolytic characteristics. This corroborated results from the cross-plot of Fl/(Fl + Py) versus Phe +

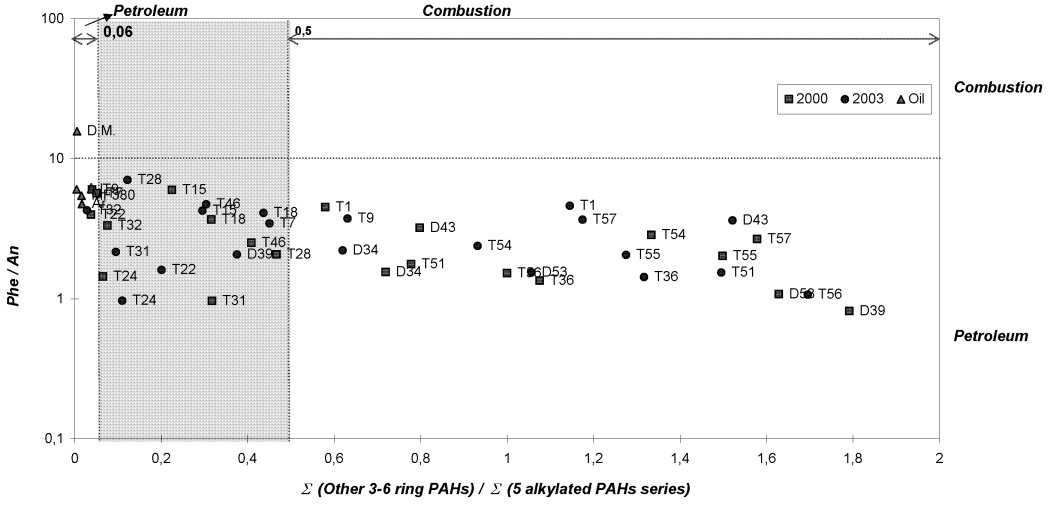

Figure 17-10 Plot of the relative ratios Σ (other 3–6-ring PAH)/Σ (5 alkylated PAH series) versus phenanthrene/anthracene for Guanabara Bay sediments from the campaigns 2000 and 2003 and MF 380, Arabian oil (AL), light oil (Ar), and diesel oil (DM). Interpretive guidelines based upon Wang et al. (1999b).

An/(Phe + An + C1Phe). Moreover, it can be seen in Figure 17-10 that the pyrogenic index included samples T7, T9, T22, T24 from the 2000 survey and T32 from the 2003 survey with clear petrogenic sources, along with analyzed oil samples. However, the ratio still showed a mixed feature for some samples within 0.06 to 0.5 values (gray-shaded area in the diagram), mainly from intertidal area.

As can be seen in Figure 17-11, a double-ratio plot of Σ (other 3–6-ring PAH)/Σ (5 alkylated PAH series) versus Fl/(Fl + Py) brought some resolution to the pyrogenic index in the range of 0.06 to 0.5 values. As shown previously, it would be expected that a predominance of petrogenic-derived sources for the samples with Fl/(Fl + Py) less than 0.4 while samples with Fl/(Fl + Py) values higher than 0.4 would show combustion characteristics. Therefore, the double-ratio Σ (other 3–6-ring PAH)/Σ (5 alkylated PAH series) versus Fl/(Fl + Py) would also confirm the contribution of petroleum in samples from the bottom left and middle quadrants of the diagram in Figure 17-11 [pyrogenic index less than 0.5 and Fl/(Fl + Py) less than 0.4: dark shaded area] and the combustion-derived sources for the samples from the top right and middle quadrants of the diagram [pyrogenic index higher than 0.06 and Fl/(Fl + Py) higher than 0.4: light shaded area]. Differently, some samples would present a mixed feature, located in the bottom right quadrant [samples T56 (surveys 2000 and 2003), D39 (survey 2000), and D53 (survey 2003)]. It can be observed that the final pattern of this corresponded reasonably to the pattern obtained from the double-ratio Fl/(Fl + Py) versus Phe + An/(Phe + An + C1Phe) of Figure 17-9, giving consistency to this study.

Another compositional index used to differentiate the natural and petrogenic PAHs was the relative perylene abundance reported by Baumard et al. (1998), which establishes the perylene abundance in relation to the 5-ring isomers, i.e., the ratio perylene/Σ (5-ring PAH = BbFl + BkFl + BaPi + BePi + DBAn) (Figure 17-12). It can be seen that the majority of samples from the intertidal region shows natural hydrocarbon contribution.

To sum up, the diagnostic ratios that exhibited a high ability to distinguish between combustion and petroleum inputs for Guanabara Bay sediments were Phe + An/(Phe + An + C1Phe) and Fl/(Fl + Py). In addition, the relative perylene abundance in relation to their 5-ring isomers also presented the ability to discriminate between natural and petrogenic

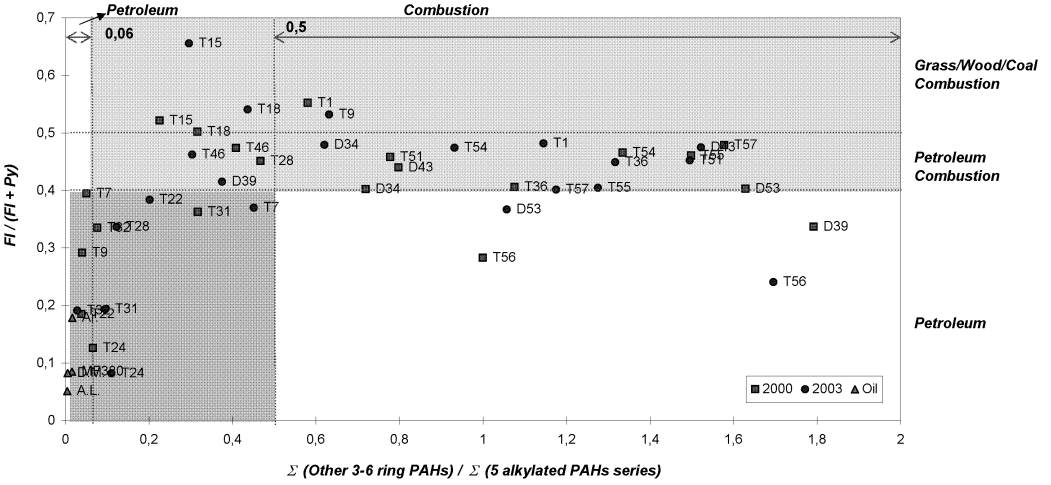

Figure 17-11 Plot of the relative ratios Σ (other 3–6-ring PAH)/Σ (5 alkylated PAH series) versus fluoranthene/(fluoranthene + pyrene) for Guanabara Bay sediments from the campaigns 2000 and 2003 and MF 380, Arabian oil (AL), light oil (Ar), and diesel oil (DM). Interpretive guidelines from Wang et al. (2002b).

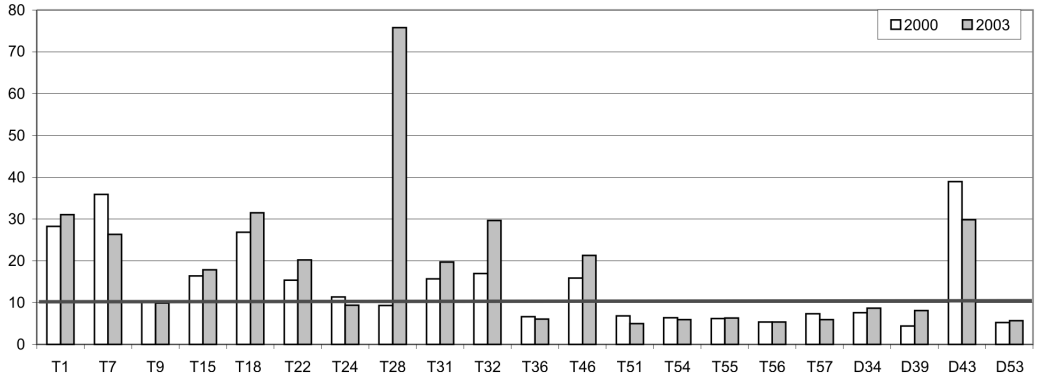

Figure 17-12 Relative perylene abundance for Guanabara Bay sediments from the campaigns 2000 and 2003.

PAH input. The PAH diagnostic ratios indicated that the Guanabara Bay sediments could be separated into three distinct groups: one with a dominant pattern and ratios consistent with petroleum-derived characteristics; another with a dominant pattern and ratios consistent with combustion-derived characteristics; and the third one with apparent mixed contributions of petrogenic and pyrolytic input.

17.3.2.2 PAH Principal Component Analysis

Figures 17-13 and 17-14 depict the factor score and factor loading results of PAH multivariate analysis of the 2000 and 2003 campaigns, respectively, in which the majority of the samples was separated into groups. In the plots, the distance and direction from the central axis have the same meaning for both samples and PAH variables.

For both campaigns, the first PCA defines two variable groups by separating alkylated PAH from parent PAH: on the left and right sides, respectively. The second PCA separates the PAHs into two groups: predominantly projected by all alkyl naphthalenes, C1 fluorenes, on the lower part; and alkyl dibenzothiophenes and alkyl phenanthrenes on the lower part (see Table 17-1 for codes).

In both datasets, the PCA model separated the sediment samples from Guanabara Bay and the four reference oils analyzed. For both campaigns, the oils projected on the lower left side of the *y*-axis with a high contribution of low-molecular-weight compounds, which are present in crudes but are usually weathered by the environment. Some samples (T7, T22, T24, T31, T32) projected on the upper left side of the *y*-axis, suggesting predominance of petrogenic input due to the contribution of alkylated phenanthrenes and dibenzothiophenes. On the other hand, other samples projected on the right side of the *y*-axis, including a group of samples with pyrolytic characteristics indicated by the dominance of high-molecular-weight compounds (T36, D43, T51, D53, T54, T55, T56, T57).

Therefore, the lower left side of the *y*-axis correlates to unweathered or less weathered oils; the upper left side correlates to samples with a more weathered petrogenic source predominance; and the lower right side correlates to samples with pyrolytic source predominance.

From one campaign to the other, it was confirmed that the class of predominant source of the samples had not significantly changed. The exceptions were T1, T7, T9, T28, T31, and D39. The intertidal samples T7 and T9 presented clear petrogenic features for the 2000 survey, corresponding to the visual inspection of the intertidal region reached by the oil after the oil spill. For the 2003 survey, the effect of the spill on these sites could no longer be an observed due mainly to the retention and cleaning effort carried out on the bay after the spill and to the natural washing capacity of the

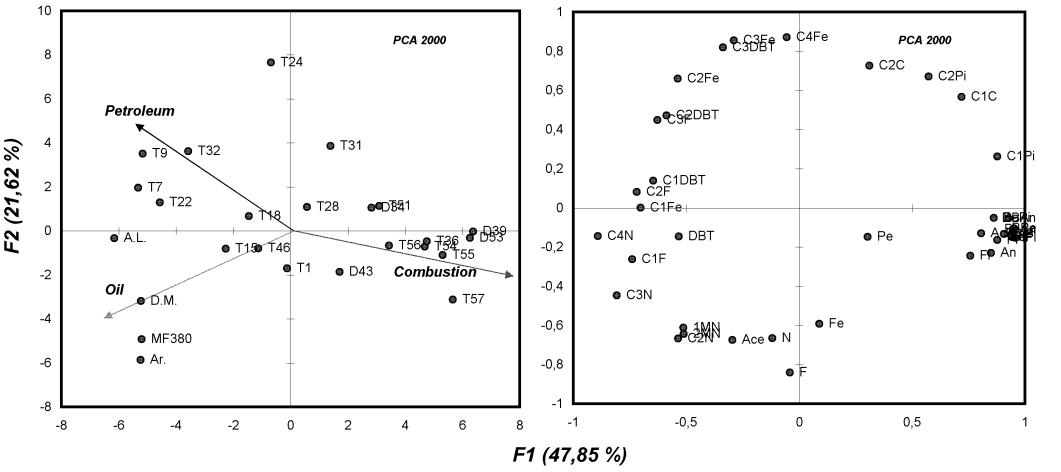

Figure 17-13 PCA projections of PAH variables and sediment samples from campaign 2000 and MF 380, Arabian oil (AL), light oil (Ar), and diesel oil (DM).

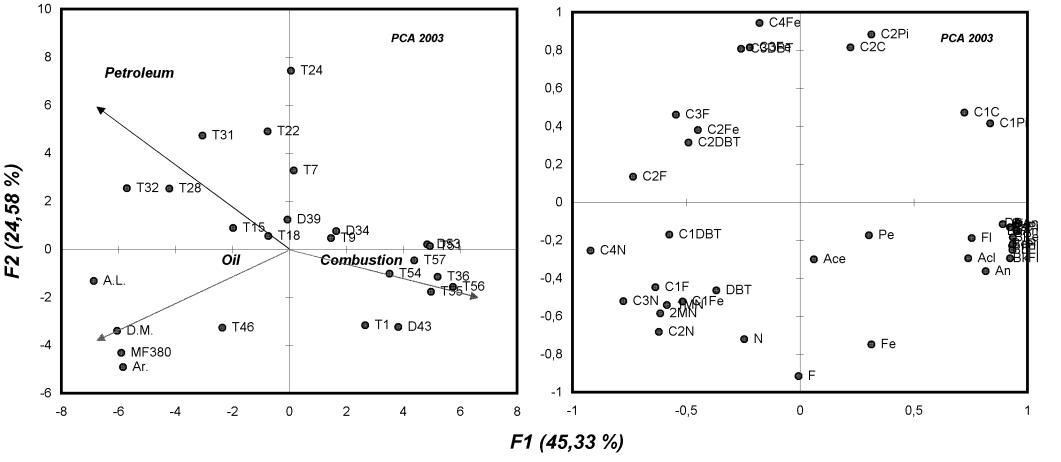

Figure 17-14 PCA projections of PAH variables and sediment samples from campaign 2003 and MF 380, Arabian oil (AL), light oil (Ar), and diesel oil (DM).

region. The full PAH pattern for these samples on the 2000 survey (Figure 17-4), with the predominance of weathered alkylated isomers, confirms this finding.

The intertidal sample T28, on the other hand, presented a clear petrogenic feature for the 2003 survey and could represent a minor independent event since its petrogenic characteristic was better revealed on the 2003 survey, having no relation to the January 2000 oil spill. The whole PAH pattern of sample T28 gives a good correlation with the PCA data, showing, in the 2003 survey, a higher concentration of weathered alkylated isomers and lower levels of four- and five-ring PAHs in relation to 2000.

For the subtidal samples T31 and D39, the change of predominant source to petrogenic features for the 2003 survey could be related to the heterogeneity of the bay sediment, also having no relation to the January 2000 oil spill.

Sample T1, on the other hand, showed a higher pyrolytic source predominance in the 2003 campaign in relation to 2000, despite its low PAH concentration. However, the whole

PAH pattern of the sample has not presented relevant differences between the two campaigns, except for an extraordinary high level of C2 naphthalenes in the 2000 survey, which could be responsible for the PCA results.

17.3.2.3 Biomarker Diagnostic Ratios

The biomarker distribution of the marine fuel MF 380 that was spilled in Guanabara Bay in January 2000 is shown in Figure 17-15. Both

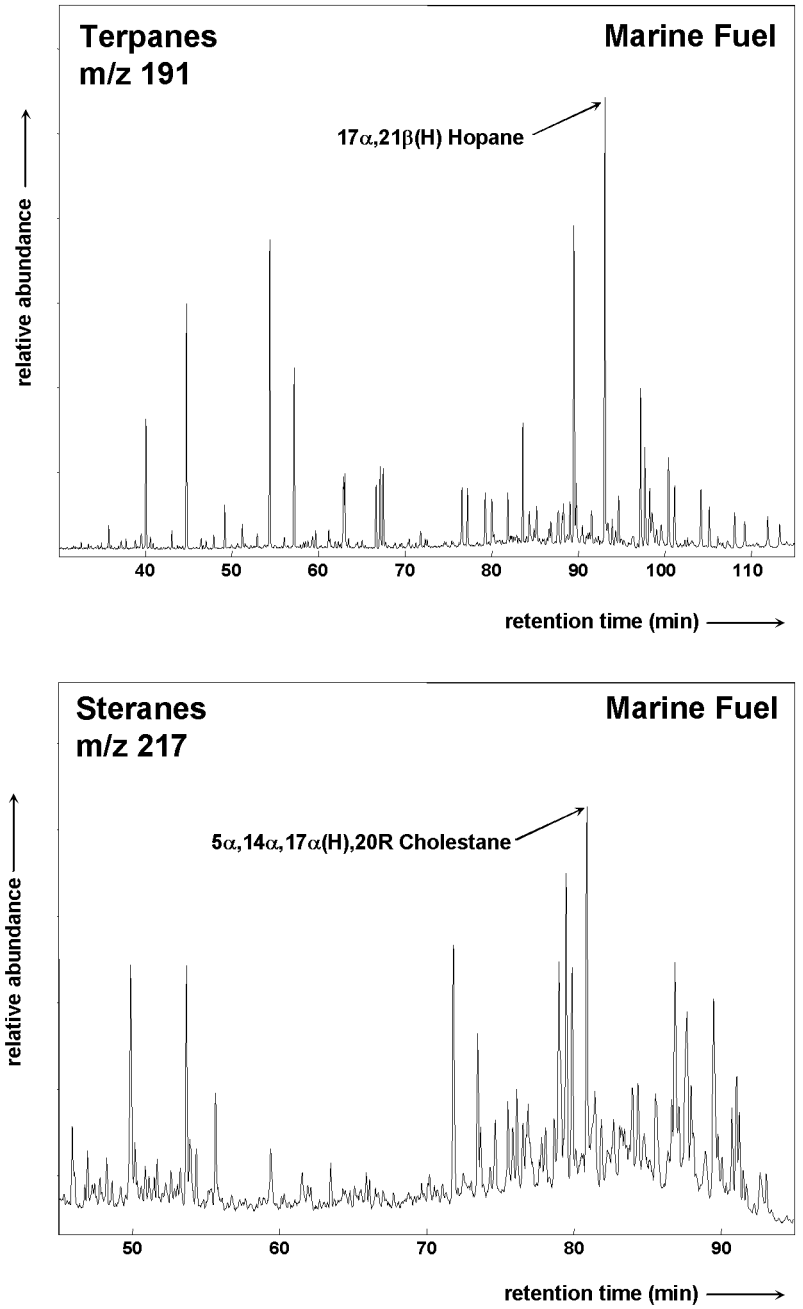

Figure 17-15 Terpane and sterane partial mass chromatograms of the spilled marine heavy fuel oil, January 2000.

Table 17-4 Results for Biomarkers, Terpanes, and Steranes of Sediment Samples from Guanabara Bay — Campaign 2000

Biomarker Ratios	*Biomarker Diagnostic Ion (m/z)*	*Intertidal*							
		T1	*T7*	*T9*	*T15*	*T18*	*T22*	*T24*	*T28*
Terpanes									
C24-tetracyclic/C26-tricyclic terpanes	**191**	0.73	0.49	0.46	0.79	0.80	0.69	0.57	0.78
gammacerane/C30-hopane	**191**	0.09	0.11	0.12	0.10	0.10	0.16	0.12	0.12
oleanane/(oleanane + C30-hopane)	**191**	0.03	0.00	0.00	0.03	0.04	0.03	0.01	0.02
(C29-hopane + C29-Ts)/C30-hopane	**191**	1.07	0.95	0.93	1.15	1.07	1.07	1.22	1.10
30-norhomohopane/(30-norhomohopane + C30-hopane)	**191**	0.097	0.066	0.068	0.104	0.088	0.120	0.089	0.103
C30-diahopane/C30-hopane	**191**	0.06	0.05	0.05	0.06	0.05	0.07	0.06	0.05
C35/C34-hopanes	**191**	1.00	0.86	0.93	0.93	0.91	0.87	0.88	0.94
C29/(C29 + C30-hopanes)	**191**	0.458	0.438	0.427	0.478	0.460	0.445	0.497	0.463
C29/C30-hopanes	**191**	0.85	0.78	0.75	0.91	0.85	0.80	0.99	0.86
hopanes/steranes	**191, 217**	7.86	6.41	6.10	6.17	5.63	5.36	7.85	6.19
tricyclic terpanes/hopanes	**191**	0.29	0.52	0.41	0.28	0.31	0.43	0.52	0.26
Ts/(Ts + Tm)	**191**	0.44	0.37	0.39	0.48	0.46	0.43	0.51	0.46
25-norhopane/C30-hopane	**177**	0.04	0.06	0.07	0.05	0.05	0.08	0.06	0.04
C29-hopane/C29-Ts	**191**	3.75	4.49	4.07	3.88	3.90	3.02	4.22	3.58
C30-35 hopanes/steranes	**191**	5.5	4.5	4.4	4.3	4.0	3.9	5.1	4.4
tetracyclic terpane polyprenoids/C27-diasteranes	**259**	0.66	0.69	0.68	0.63	0.59	0.69	0.79	0.62
Steranes									
% C27 5α,14β,17β(H),20S	**218**	32	40	39	31	31	34	36	33
% C28 5α,14β,17β(H),20S	**218**	24	23	25	27	28	27	23	25
% C29 5α,14β,17β(H),20S	**218**	44	37	37	42	41	39	41	42
C27/C29 5α,14β,17β(H),20S	**218**	0.72	1.09	1.05	0.74	0.75	0.87	0.86	0.77
C28/C29 5α,14β,17β(H),20S	**218**	0.55	0.63	0.67	0.63	0.69	0.71	0.55	0.59
C21 + C22/total steranes	**217**	0.09	0.09	0.07	0.09	0.10	0.10	0.08	0.07
C27 diasteranes/regular steranes	**217**	0.62	0.45	0.57	0.65	0.65	0.63	0.85	0.52
C29 5α,14α,17α(H) 20S/20S + 20R	**217**	0.51	0.53	0.54	0.50	0.50	0.53	0.64	0.48
C29 5α,14β,17β(H)/5α,14β,17β(H) + 5α,14α,17α(H)	**217**	0.53	0.46	0.48	0.54	0.53	0.47	0.41	0.53
C29/C27 5α,14α,17α(H),20S	**217**	0.55	0.54	0.53	0.55	0.56	0.61	0.74	0.54

terpane and sterane profiles are typical of a crude oil derived from a saline lacustrine depositional environment from the Brazilian marginal basins (Mello et al., 1988a, 1988b; Peters et al., 2005). The main molecular features are expressed by the following biomarker ratios: hopanes/steranes 6.3; tricyclic terpanes/hopanes 0.91; Ts/(Ts + Tm) 0.30; gammacerane/hopane 0.13; 30-norhopane/hopane 0.72; TPP/C27-diasteranes 0.70; C27-diasteranes/C27-regular steranes 0.72; 25-norhopane/C30-hopane 0.09; and C29-steranes 20S/20S + 20R 0.53.

Biomarker data for the sediment samples are presented in Tables 17-4 and 17-5. Based on selected biomarker ratios, it was observed that

Subtidal												
T31	*T32*	*T36*	*T46*	*T51*	*T54*	*T55*	*T56*	*T57*	*D34*	*D39*	*D43*	*D53*
0.71	0.72	0.77	0.79	0.81	0.86	0.72	0.84	0.76	0.81	0.77	0.72	0.86
0.13	0.10	0.10	0.10	0.10	0.07	0.09	0.10	0.10	0.10	0.08	0.09	0.08
0.02	0.01	0.03	0.04	0.03	0.05	0.03	0.04	0.03	0.03	0.08	0.03	0.08
1.22	1.04	1.08	1.10	1.09	0.90	1.10	1.07	1.15	1.08	0.93	1.10	0.99
0.119	0.100	0.095	0.099	0.107	0.061	0.094	0.117	0.095	0.093	0.059	0.087	0.078
0.06	0.05	0.05	0.05	0.05	0.05	0.05	0.05	0.06	0.05	0.06	0.05	0.07
0.88	0.83	0.94	0.91	0.88	0.84	0.93	0.95	0.88	0.92	0.84	0.92	0.92
0.487	0.435	0.462	0.466	0.456	0.414	0.467	0.447	0.482	0.461	0.423	0.467	0.441
0.95	0.77	0.86	0.87	0.84	0.71	0.88	0.81	0.93	0.86	0.73	0.87	0.79
6.59	6.33	7.66	7.12	7.05	7.07	7.98	6.45	6.75	7.10	5.34	8.44	5.91
0.44	0.31	0.27	0.30	0.25	0.24	0.28	0.26	0.30	0.29	0.33	0.22	0.32
0.47	0.48	0.47	0.47	0.40	0.45	0.48	0.45	0.48	0.46	0.40	0.39	0.43
0.05	0.04	0.03	0.03	0.04	0.04	0.03	0.04	0.03	0.04	0.06	0.04	0.04
3.55	2.82	3.87	3.79	3.27	3.67	3.98	3.05	4.16	3.79	3.67	3.97	3.95
4.4	4.4	5.3	4.9	4.9	5.0	5.4	4.6	4.6	4.9	3.7	6.0	4.1
0.66	0.63	0.64	0.62	0.64	0.59	0.63	0.60	0.63	0.64	0.62	0.63	0.63
35	32	28	27	27	27	28	29	29	29	26	31	27
24	26	26	27	28	28	26	29	26	25	34	26	31
41	42	46	46	45	45	46	43	45	46	41	43	42
0.84	0.76	0.61	0.60	0.60	0.61	0.61	0.66	0.65	0.64	0.63	0.72	0.64
0.58	0.60	0.58	0.59	0.63	0.62	0.56	0.66	0.58	0.54	0.82	0.60	0.75
0.09	0.06	0.08	0.09	0.07	0.08	0.08	0.08	0.08	0.08	0.10	0.07	0.10
0.69	0.47	0.90	0.87	0.59	0.58	0.92	0.74	0.54	0.74	1.08	0.59	1.20
0.51	0.42	0.54	0.52	0.49	0.45	0.49	0.47	0.50	0.51	0.55	0.49	0.56
0.51	0.47	0.55	0.56	0.51	0.51	0.56	0.51	0.56	0.55	0.57	0.55	0.56
0.57	0.58	0.63	0.56	0.58	0.60	0.57	0.60	0.56	0.55	0.57	0.54	0.59

samples taken from the same site in both campaigns, 2000 and 2003, are very similar. An example is sample T24 sampled in both campaigns. Sample T24 presents a higher value for C29/C27 5α,14α,17α(H),20S sterane ratio compared to the other samples, 0.74 and 0.81, for campaigns 2000 and 2003, respectively (Figure 17-16). Such molecular features result in an uncommon sterane distribution showing a predominance of C27-sterane 5α,14β, 17β(H),20S in sample T24.

In general, most of the samples from Guanabara Bay have not shown any correlation with the spilled marine fuel. There were a few exceptions such as two intertidal samples, T7 and T9, from the campaign 2000, that showed

Table 17-5 Results for Biomarkers, Terpanes, and Steranes of Sediment Samples from Guanabara Bay — Campaign 2003 the 30-Norhopane Series

Biomarker Ratios	*Biomarker Diagnostic Ion (m/z)*	*Intertidal*			*Subtidal*				
		T9	*T15*	*T24*	*T31*	*T32*	*T51*	*T57*	*D39*
Terpanes									
C24-tetracyclic/C26-tricyclic terpanes	**191**	0.57	0.73	0.57	0.83	0.86	0.75	0.81	0.81
Gammacerane/C30-hopane	**191**	0.12	0.11	0.19	0.11	0.09	0.11	0.10	0.12
Oleanane/(oleanane + C30-hopane)	**191**	0.01	0.02	0.00	0.01	0.01	0.04	0.04	0.01
(C29-hopane + C29-Ts)/C30-hopane	**191**	1.09	1.10	1.34	1.18	1.13	1.07	1.06	1.12
30-Norhomohopane/(30-norhomohopane + C30-hopane)	**191**	0.08	0.10	0.12	0.10	0.09	0.09	0.10	0.10
C30-diahopane/C30-hopane	**191**	0.07	0.05	0.10	0.05	0.05	0.06	0.06	0.06
C35/C34-hopanes	**191**	0.88	0.95	0.86	0.91	0.85	0.89	0.86	0.90
C29/(C29 + C30-hopanes)	**191**	0.46	0.46	0.51	0.48	0.47	0.46	0.45	0.46
C29/C30-hopanes	**191**	0.88	0.87	1.06	0.95	0.92	0.85	0.84	0.88
Hopanes/steranes	**191, 217**	8.26	7.42	7.62	7.30	6.89	8.01	7.96	7.09
Tricyclic terpanes/hopanes	**191**	0.35	0.34	0.73	0.31	0.28	0.29	0.25	0.27
Ts/(Ts + Tm)	**191**	0.45	0.47	0.53	0.48	0.49	0.48	0.48	0.50
25-norhopane/C30-hopane	**177**	0.05	0.04	0.09	0.03	0.03	0.03	0.03	0.03
C29-hopane/C29-Ts	**191**	4.14	3.76	3.69	4.21	4.35	3.90	3.81	3.73
C30-35 hopanes/steranes	**191**	5.9	5.2	4.8	5.0	4.7	5.7	5.7	4.98
Tetracyclic terpane polyprenoids/ C27-diasteranes	**259**	0.68	0.62	0.85	0.61	0.60	0.66	0.67	0.62
Steranes									
% C27 5α,14β,17β(H),20S	**218**	31	31	34	32	32	27	26	33
% C28 5α,14β,17β(H),20S	**218**	26	26	24	24	24	28	27	25
% C29 5α,14β,17β(H),20S	**218**	43	43	42	44	44	45	47	42
C27/C29 5α,14β,17β(H),20S	**218**	0.71	0.71	0.82	0.73	0.73	0.59	0.56	0.80
C28/C29 5α,14β,17β(H),20S	**218**	0.60	0.59	0.59	0.54	0.54	0.62	0.57	0.59
C21 + C22/total steranes	**217**	0.08	0.12	0.08	0.09	0.09	0.08	0.08	0.08
C27 diasteranes/regular steranes	**217**	0.96	0.92	1.27	0.75	0.67	1.12	0.91	0.80
C29 5α,14α,17α(H) 20S/20S + 20R	**217**	0.57	0.53	0.73	0.43	0.41	0.53	0.49	0.47
C29 5α,14β,17β(H)/5α,14β,17β(H) + 5α,14α,17α(H)	**217**	0.54	0.57	0.37	0.54	0.54	0.57	0.58	0.55
C29/C27 5α,14α,17α(H),20S	**217**	0.55	0.54	0.81	0.51	0.52	0.60	0.55	0.52

a slight correlation with the marine fuel oil spilled (Figure 17-17). Sample D43, from campaign 2000, presented a higher input of recent organic matter compared to other samples. Consequently, its mass chromatograms *m/z* 191 and 217 showed some interfering peaks.

On the other hand, there is a good biomarker correlation for most of the samples to petroleums derived from a marine carbonate depositional environment. The main features of this kind of crude oil are high values for the C29/C30-hopane and C35/C34-hopane ratios, ranging from 0.85 up to 1.10, the presence of oleanane, high values for the C24-tetracyclic/C26-tricyclic terpane ratio, ranging from 0.57 up to 0.86, values lower than 7.0 for the hopane/sterane ratio, and the presence of Table 17-5. On the other hand, the spilled fuel presents lower values for C29/C30-hopane and C35/C34-hopane ratios, ranging from 0.70 up to 0.86, the absence of oleanane, a lower value for the C24-tetracyclic/C26-tricyclic terpane ratio, 0.40, very low relative abundance or even absence of 30-norhopane series (Figure 17-18). Sterane distributions of sediment samples showed also a significant similarity to those of marine carbonate oils. Based on specific sterane ratios, such as C27/C29 5α,14β,17β(H),20S, C28/C29 5α,14β,17β(H),20S, and C29/C27 5α,

Figure 17-16 A plot of C27/C29-steranes 5α,14β,17β(H),20S against C29/C27-steranes 5α,14α,17α(H),20S showing the similarity between most of the samples and the correlation between both samples T24 collected in campaigns 2000 and 2003.

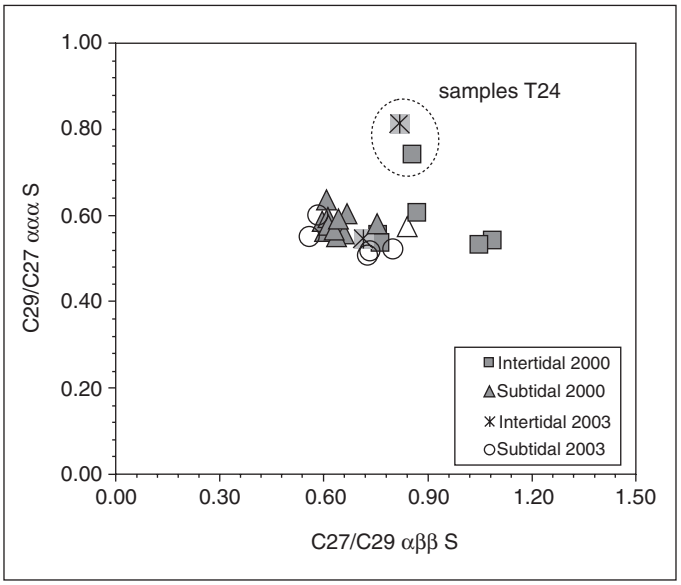

Figure 17-17 A plot of C24-tetracyclic/C26-tricyclic terpanes against C29/(C29 + C30-hopanes) highlighting the correlation between the marine fuel and samples T7 and T9 from the campaign 2000.

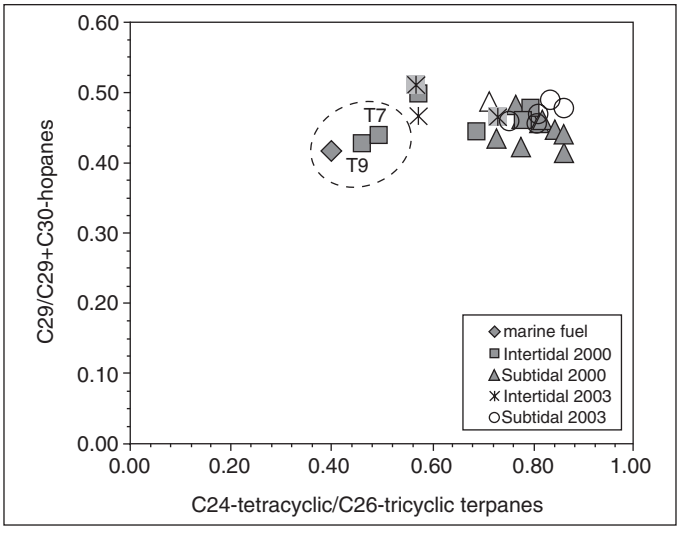

Figure 17-18 A plot of Ts/(Ts + Tm) against 30-norhomohopane/(30-norhomohopane + hopane) showing the correlation between samples and a marine carbonate-sourced crude oil.

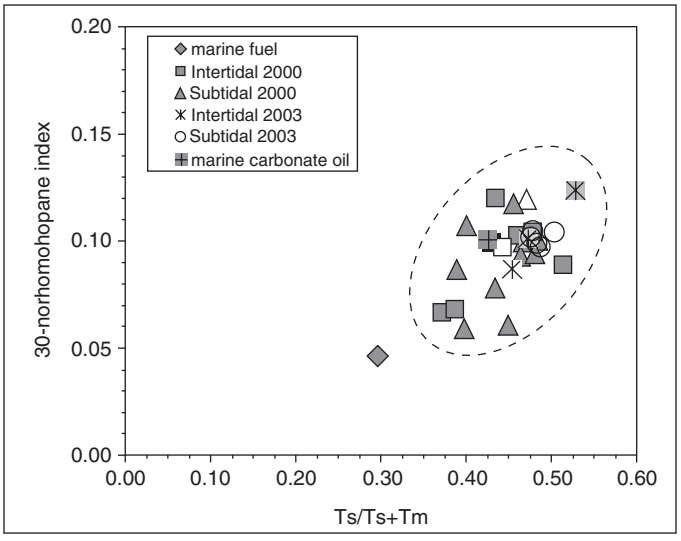

14α,17α(H),20S, this correlation can be observed (Figures 17-19 and 17-20).

17.4 Conclusions

Parent and alkyl PAH (a total of 38 compounds) and biomarker terpanes and steranes have been quantified in 21 sediment samples from a highly urban and industrialized ecosystem, the Guanabara Bay, Rio de Janeiro, Brazil. The study was carried out in two campaigns; the first immediately after the oil spill accident in January 2000, and the second, three years later. The sampling design included areas potentially affected and unaffected by the spilled oil, covering the entire ecosystem. The difference in PAH concentrations between the 2000 and 2003 samples was not statistically significant, reflecting the continued chronic anthropogenic pollution of the bay, which was similar to various international estuarine sites. The similarity of Guanabara Bay PAH levels could also be confirmed by comparing the data from both the 2000 and 2003 surveys with pre-

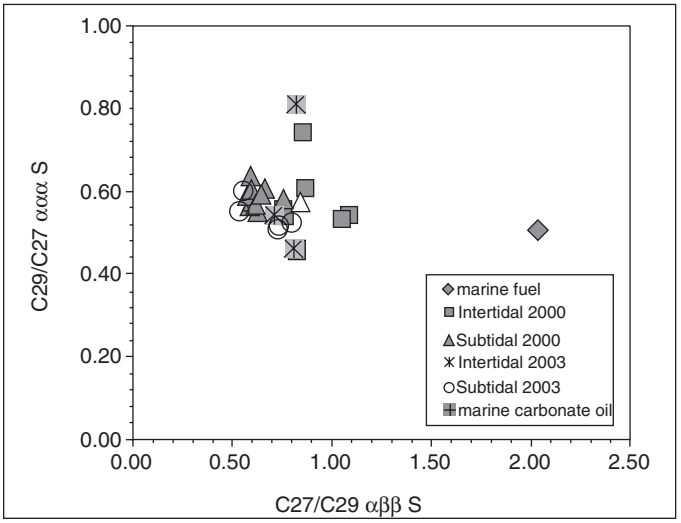

Figure 17-19 A plot of C27/C29-steranes 5α,14β,17β(H),20S against C29/C27-steranes 5α,14α,17α(H),20S showing the correlation between most of the samples and a marine carbonate-sourced crude oil.

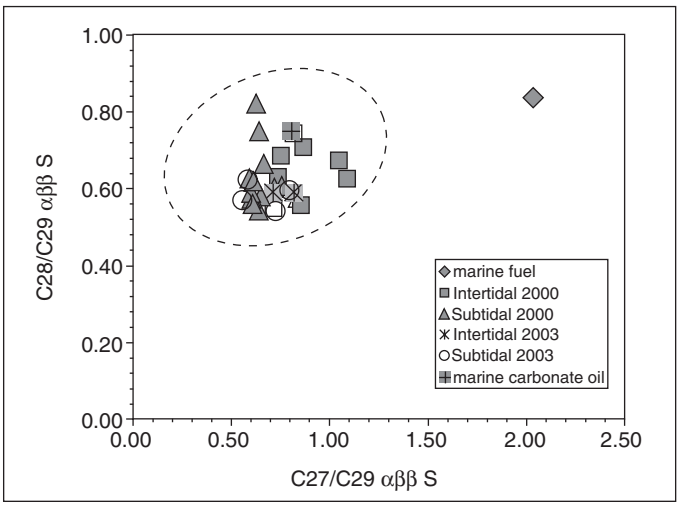

Figure 17-20 A plot of C27/C29-steranes 5α,14β,17β(H),20S against C28/C29-steranes 5α,14β,17β(H),20S showing the correlation between the sediment samples and a marine carbonate-sourced crude oil.

vious PAH data observed in the bay, which were in the same range.

The hydrocarbon source indications were made by using PAH ratios for the samples studied. Some diagnostic ratios exhibited a higher ability to distinguish combustion- and petroleum-derived PAH inputs for Guanabara Bay sediments, namely

Phenanthrene + anthracene/(phenanthrene + anthracene + C1phenanthrene)
Fluoranthene/(fluoranthene + pyrene)
Σ (other 3–6-ring PAHs)/Σ (5 alkylated PAH series)

In addition, the relative perylene abundance in relation to their 5-ring isomers also presented the ability to recognize a contribution from natural (biogenic) PAH input.

Furthermore, the PCA results also exhibited a promising capacity to separate the samples into groups, proving to be a helpful tool for PAH source identification in the environment, corroborating the diagnostic indexes. The results indicated clear patterns of dominantly petrogenic and dominantly pyrolytic hydrocarbons inflow to the bay.

Summarizing, the PAH sources to Guanabara Bay sediments can be separated into groups:

- samples with a clear pattern of petrogenic input — the majority located near the vicinity of the accident in January 2000;
- samples with combustion characteristics — those from the majority of subtidal stations;
- samples without a clear contribution of petrogenic or pyrolytic input, i.e., mixed sources.

A biogenetic contribution was also confirmed for most intertidal samples and for some subtidal samples.

In addition, no significant temporal changes were confirmed for the class of predominant sources in the samples in this study, revealing that the PAH concentrations in Guanabara Bay sediments are not obviously related to the oil spill event, but rather to long-term anthropogenic input. Furthermore, this result can also indicate that there was no significant impact of the oil spill of January 2000 into the Guanabara Bay sediments.

Based on biomarker data, it was observed that most of the sediments from Guanabara Bay have not shown any correlation with the spilled marine heavy fuel oil, except two samples that showed a slight correlation with the spilled fuel. Instead, the sediment samples collected in both campaigns showed a clear input of oils derived from a marine carbonate depositional environment, reflecting chronic anthropogenic pollution of the bay. The spilled MF 380 oil was produced from a Brazilian lacustrine oil that shows a different biomarker distribution pattern in comparison with the oils derived from a marine carbonate depositional environment.

Still more investigation seems to be necessary since Guanabara Bay is in a complex urban area with a significant anthropogenic hydrocarbon introduction process. Currently, a multidisciplinary project in Guanabara Bay is being carried out at the Petrobras Research Center, taking into account not only diagnostic hydrocarbon ratios but also geochemical biomarkers, individual compound carbon isotopic ratios, contaminants such as pesticides and coprostanol, contaminant normalized concentration to organic carbon or grain size distribution, ecotoxicity essays, and benthonic community evaluation, among others.

Acknowledgments

Field surveys were carried out by Federal Fluminense University and Petrobras SA, Brazil. Analyses of sediment samples for PAH were performed by PUC–Catholic University, and the biomarkers were performed by Petrobras SA, Brazil. The authors are grateful to Carlos German Massone of Gorceix Foundation, Dr. Arthur de Lemos Scofield of PUC–Catholic University, and Dr. Valter Jose Fernandes Junior of Federal University of Rio Grande do Norte, Brazil, for their participation in this study and would like to thank Andre Luiz dos Santos Brites and Rui Alexandre Oliveira da Fonseca for helping with the artwork for the chapter. The authors also wish to acknowledge

Dr. J. Michael Moldowan, Mauro Rocha Evangelho, and Irene Terezinha Gabardo for their constructive comments on the chapter.

References

Amador, E.S., Baia de Guanabara e ecossistemas periféricos: Homem e natureza, *Edição do Autor*, Rio de Janeiro, Brazil, 1997, pp. 148–159.

Anderson, J.W., F.C. Newton, J. Hardin, R.H. Tukey, and K.E. Richter, Chemistry and toxicity of sediments from San Diego Bay, including a biomarker (P450 RGS) response, *In: Environmental Toxicology and Risk Assessment: Biomarkers and Risk Assessment*, D.A. Bengtson and D.S. Henshel (eds.), Philadelphia, USA: American Society for Testing and Materials, 1996, **5,** 53–78.

Baumard, P., H. Budzinski, Q. Mchin, P. Garrigues, T. Burgeot, and J. Bellocq, Origin and bioavailability of PAH in Mediterranean Sea from mussel and sediment records, *Estuarine, Coastal and Shelf Sci.*, 1998, **47**, 77–90.

Bixian, M., F. Jiamo, Z. Gan, L. Zheng, M. Yushun, S. Guoying, and W. Xingm, Polycyclic aromatic hydrocarbons in sediments from the Pearl River and estuary, China: Spatial and temporal distribution and sources, *Appl. Geochem.*, 2001, **16**, 1429–1445.

Bentz, C.M. and F.P. Miranda, Application of remote sensing data for oil spill monitoring in the Guanabara Bay, Rio de Janeiro, Brazil, *Proc. Intl. Geosci. Remote Sensing Symp.*, 2001 Sydney, Australia.

Brown, D.W., B.B. McCain, B.H. Hornes, C.A. Sloan, K.L. Tilbury, S.M. Pierce, D.G. Burrows, S.-L. Chan, J.T. Landahl, and M.M. Krahn, Status, correlations and temporal trends of chemical contaminants in fish and sediment from selected sites on the Pacific Coast of the USA, *Mar. Poll. Bull.*, 1998, **37**(1–2), 67–85.

Budzinki, H., I. Jones, J. Bellocq, C. Piérard, and P. Garrigues, Evaluation of sediment contamination by polycyclic aromatic hydrocarbons in the Gironde Estuary, *Mar. Chem.*, 1997, **48**, 85–97.

Chalaux, N., Dinamica costanera de les aportations contaminants presents als efluents urbans, Universidade de Barcelona, Spain, 1995.

Colombo, J.C., Biogeochemical assessment of the 1999 Rio de la Plata oil spill, *Proc. Seventh Latin American Cong. Org. Geochem.*, Foz do Iguaçu, Brazil, 2000.

Colombo, J.C., E. Pelletier, C. Brochu, and M. Khalil, Determination of hydrocarbon sources using *n*-alkane and polyaromatic hydrocarbon indexes. Case Study: Rio de la Plata Estuary, Argentina, *Environ. Sci. Tech.*, 1989, **23**, 888–894.

Eglinton, G. and M. Calvin, Chemical fossils, *Sci. Amer.*, 1967, **261**, 32–43.

Eglinton, G., P.M. Scott, T. Besky, A.L. Burlingame, and M. Calvin, Hydrocarbons of biological origin from a one-billion-year-old sediment, *Science*, 1964, **145**, 263–264.

Elias, V.O., B.R.T. Simoneit, and J.N. Cardoso, Levoglucosan, a molecular fossil as indicator of biomass burning contribution in sediments of the Amazon Shelf, *Proc. Seventh Latin-American Congress on Org. Geochem.*, Foz do Iguaçu, Brazil, 2000, pp. 243–244.

EPA-3540, Soxhlet extraction, *In*: *Test Method for Evaluation Solid Waste Physical/Chemical Methods, Laboratory Manual*, Washington, DC: Environmental Protection Agency, 1986, v. I-B.

EPA-3630C, Silica gel clean-up, *In*: *Test Method for Evaluation Solid Waste Physical/Chemical Methods, Laboratory Manual*, Washington, DC: Environmental Protection Agency, 1986, Rev. 3.

EPA-8270C, Gas chromatography/mass spectrometry for semi-volatile organics capillary column technique. *In*: *Test Method for Evaluation Solid Waste Physical/Chemical Methods, Laboratory Manual*, Washington, DC: Environmental Protection Agency, 1986, v. I-B.

FEEMA, Qualidade de Água da Baía de Guanabara, Programa de Despoluição da Baía de Guanabara — Programas Ambientais Complementares 1998.

FEEMA, www.feema.rj.gov.br. Accessed on 08/01/2003.

Fu, J., Z. Wang, B. Mai, and Y. Kang, Field monitoring of toxic of organic pollution in sediments of Pearl River Estuary and its tributaries, *Water Sci. Tech.*, 2001, **43**, 83–89.

Fung, C.N., G.J. Zheng, D.W. Connell, X. Zhang, H.L. Wong, J.P. Giesy, Z. Fang, and P.K.S. Lam, Risks posed by trace organic contaminants in coastal sediments in the Pearl River Delta, China, *Mar. Poll. Bull.*, 2005, **50**(10), 1036–1049.

Gschwend, P.M. and R.A. Hites, Fluxes of polycyclic aromatic hydrocarbons to marine and lacustrine sediments in the Northeastern United States, *Geochimica et Cosmochimica Acta*, 1981, **45**, 2359–2367.

Hamacher, C., Determinação de hidrocarbonetos em amostras de água e sedimento da Baía de

Guanabara, M.Sc. Thesis, Catholic University PUC-Rio, Chemistry Department, Brazil, 1996.

Hites, R.A. and W.G. Biemann, Identification of specific organic compounds in a highly anoxid sediment by CG/MS and HRMS, *Adv. Chem. Ser.*, 1975, **147**, 188–201.

Holba, A.G., L. Ellis, E. Tegelaar, M.S. Singletary, and P. Albrecht, Tetracyclic polyprenoids: Indicators of fresh water (lacustrine) algal input, *Geol.*, 2000, **28**(3), 251–254.

Holba, A.G., L.I. Dzou, G.D. Wood, L. Ellis, P. Adam, P. Schaeffer, P. Albrecht, T. Greene, and W.B. Hughes, Application of tetracyclic polyprenoids as indicators of input from fresh-brackish water environments, *Org. Geochem.*, 2003, **34**(3), 441–469.

Kayal, S.I. and D.W. Connell, Occurrence and distribution of polycyclic aromatic hydrocarbons in surface sediments and water from the Brisbane River Estuary, Australia, *Estuarine Coastal and Shelf Sci.*, 1989, **29**, 473–487.

Ke, L., T.W.Y. Wong, Y.S. Wong, and N.F.Y. Tam, Fate of polycyclic aromatic hydrocarbon (PAH) contamination in a mangrove swamp in Hong Kong following an oil spill, *Mar. Poll. Bull.*, 2002, **45**, 339–347.

Kennicutt II, M.C., T.L. Wadw, B.J. Presley, A.G. Requejo, J.M. Brooks, and G.J. Denoux, Sediment contaminants in Casco Bay, Maine: Inventories, source and potential for biological impact, *Environ. Sci. Tech.*, 1994, **28**(1), 1–15.

Kennicutt II, M.C. (ed.), Gulf of Mexico offshore operations monitoring experiment; final report, U.S. Department of the Interior Minerals Management Service, Gulf of Mexico OCS Region, New Orleans; USA, 1995, p. 700.

Kjerfve, B., C.H.A. Ribeiro, G.T.M. Dias, A.M. Fillippo, and V.S. Quaresma, Oceanographic characteristics of an impacted coastal bay: Baía de Guanabara, *Continental Shelf Res.*, 1997, **17**(13), 1609–1643.

Khim, J.S., K. Kannan, D.L. Villeneuve, C.H. Koh, and J.P. Giesy, Characterization and distribution of trace organic contaminants in sediment from Masan Bay, Korea, 1. Instrumental analysis, *Environ. Sci. Tech.*, 1999, **33**, 4199–4205.

Lima, A.L.C., Geocronologia de hidrocarbonetos poliaromáticos (PAH) — Estudo de caso: Baía de Guanabara, M.Sc. Thesis, Catholic University PUC-Rio, Chemistry Department, Brazil, 1996.

Lipatou, E. and J. Albaigés, Atmospheric deposition of hydrophobic organic chemicals in the Northwestern Mediterrean Sea: Comparison with the Rhone River input, *Mar. Chem.*, 1994, **46**, 153–164.

Mayr, L.M., Avaliação ambiental da Baía de Guanabara com o suporte do geoprocessamento. Ph.D. Thesis, Rio de Janeiro Federal University — UFRJ, Geoscience Institute, Brazil, 1998.

Mello, M.R., P.C. Gaglianone, and J.R. Maxwell, Geochemical and biological marker assessement of depositional environments using Brazilian offshore oils, *Mar. Petrol. Geol.*, 1998a, **5**, 205–223.

Mello, M.R., N. Telnaes, and P.C. Gaglianone, Organic geochemical characterization of depositional paleoenvironments in Brazilian marginal basins, *Org. Geochem.*, 1998b, **13**, 31–46.

Meniconi, M.F.G., I.T. Gabardo, M.E.R. Carneiro, S.M. Barbanti, G.C. Silva, and C.G. Massone, Brazilian oil spills chemical characterization — case studies, *Environ. Forensics*, 2002, **3**(3/4), 303–321.

Neff, J., *Bioaccumulation in Marine Organisms*, 2nd ed., Elsevier, 1st ed., UK, 2002, pp. 269–277.

Pereira, W.E., F.D. Hostettler, and J.B. Rapp, Distributions and fate of chlorinated pesticides, biomarkers and polycyclic aromatic hydrocarbons in sediments along a contamination gradient from a point-source in San Francisco Bay, California, *Mar. Environ. Res.*, 1996, **41**, 299–314.

Peters, K.E., C.C. Walters, and J.M. Moldowan, *The Biomarker Guide*, 1st ed., Cambridge University Press, 2nd ed., UK, 2005.

Philp, R.P., Fossil fuel biomarkers: Application and spectra, *Methods in Geochem. Geophys.*, 1985, **23**.

Readman, J.W., M.R. Preston, and R.F.C. Mantoura, An integrated technique to quantify sewage, oil and PAH pollution in estuarine and coastal environments, *Mar. Poll. Bull.*, 1998, **17**, 298–308.

Readman, J.W., G. Fillman, I. Tolosa, J. Bartocci, J.P. Villeneuve, C. Catinni, and L.D. Mee, Petroleum and PAH contamination of the Black Sea, *Mar. Poll. Bull.*, 2002, **44**, 48–62.

Sherblom, P.M., D. Kelly, and R.H. Pierce, Baseline survey of pesticide and PAH concentrations from Sarasota Bay, Florida, USA, *Mar. Poll. Bull.*, 1995, **30**, 568–673.

Sicre, M.A., J.C. Marty, A. Saliot, X. Aparicio, J. Grimalt, and J. Albaige, Aliphatic and aromatic hydrocarbons in different sized aerosols over the Mediterranean Sea: Occurrence and origin, *Atmos. Environ.*, 1987, **21**, 2247–2259.

Stout, S.A., V.S. Mager, R.M. Uhler, J. Ickes, J. Abbott, and R. Brenne, Characterization of

naturally occurring and anthropogenic PAHs in urban sediments — Wycoff/Eagle Harbour superfund site, *Environ. Forensics*, 2001, **2**, 287–300.

Stout, S.A., A.D. Uhler, and S.D. Emsbo-Mattingly, Comparative evaluation of background anthropogenic hydrocarbons in surficial sediments from nine urban waterways, *Environ. Sci. Tech.*, 2004, **38**, 2987–2994.

Tam, N.F.Y., L. Ke, X.H. Wang, and Y.S. Wong, Contamination of polycyclic aromatic hydrocarbons in surface sediments of mangroves swamps, *Environ. Poll.*, 2001, **114**, 255–2631.

Wang, Z., M. Fingas, and D.S. Page, Oil spill identification, *J. Chrom. A*, 1999a, **843**, 369–411.

Wang, Z., M. Fingas, Y.Y. Shu, L. Sigouin, M. Landriault, and P. Lambert, Quantitative characterization of PAHs in burn residue and soot samples and differentiation of pyrogenic PAHs from petrogenic PAHs — the 1994 mobile burn study, *Environ. Sci. Tech.*, 1999b, **33**, 3100–3109.

Witt, G. and H. Siegel, The consequences of the Oder Flood in 1997 on the distribution of polycyclic aromatic hydrocarbons (PAHs) in the Oder River Estuary, *Mar. Poll. Bull.*, 2000, **40**(12), 1124–1131.

Wu, Y., J. Zhang, and Z. Zhu, Polycyclic aromatic hydrocarbons in the sediments of the Yalujiang Estuary, North China, *Mar. Poll. Bull.*, 2003, **46**, 619–625.

Xu, S., X. Gao, M. Liu, and Chen, China's Yangtze Estuary II — phosphorus and polycyclic aromatic hydrocarbons in tidal flat sediments, *Geomorph.*, 2001, **41**, 207–217.

Yim, U.H., S.H. Hong, W.J. Shim, J.R. Oh, and M. Chang, Spatio-temporal distribution and characteristics of PAHs in sediments from Masan Bay, Korea, *Mar. Poll. Bull.*, 2005, **50**, 319–326.

Youngblood, W.W. and M. Blumer, Polycyclic aromatic hydrocarbons in Gulf of Maine sediments and Nova Scotia soils, *Geochimica et Cosmochimica Acta*, 1975, **38**, 303–1314.

Yunker, M.B., R.W. MacDonald, R. Brewer, S. Sylvestre, T. Tuominen, M. Sekela, R.H. Mitchell, D.W. Paton, B.R. Fowler, C. Gray, D. Goyette, and D. Sullivan, Assessment of natural and anthropogenic hydrocarbon inputs using PAHs as tracers, The Fraser River Basin and Strait of Georgia 1987–1997, *Report DOE FRAP*, Vancouver; BC: Environment Canada and Fisheries and Oceans Canada, 2000, p. 128.

Yunker, M.B., R.W. MacDonald, R. Brewer, R. Vingarzan, R.H. Mitchell, D. Goyette, and S. Sylvestre, PAHs in the Fraser River Basin: A critical appraisal of PAH ratios as indicators of PAH source and composition, *Org. Geochem.*, 2002, **33**, 489–515.

Zhang, Z.L., H.S. Homg, J.L. Zhou, and G. Yu, Phase association of polycyclic aromatic hydrocarbons in the Minjiang River Estuary, China, *The Science of the Total Environment*, 2004, **323**, 71–86.

Zhang, J., L. Cai, D. Yuan, and M. Chen, Distribution and sources of polynuclear aromatic hydrocarbons in mangrove surficial sediments of Deep Bay, China, *Mar. Poll. Bull.*, 2004, **49**, 479–486.

Zhou, J.L. and K. Maskaoui, Distribution of polycyclic aromatic hydrocarbons in water and surface sediments from Daya Bay, China, *Environ. Poll.*, 2003, **121**, 269–281.